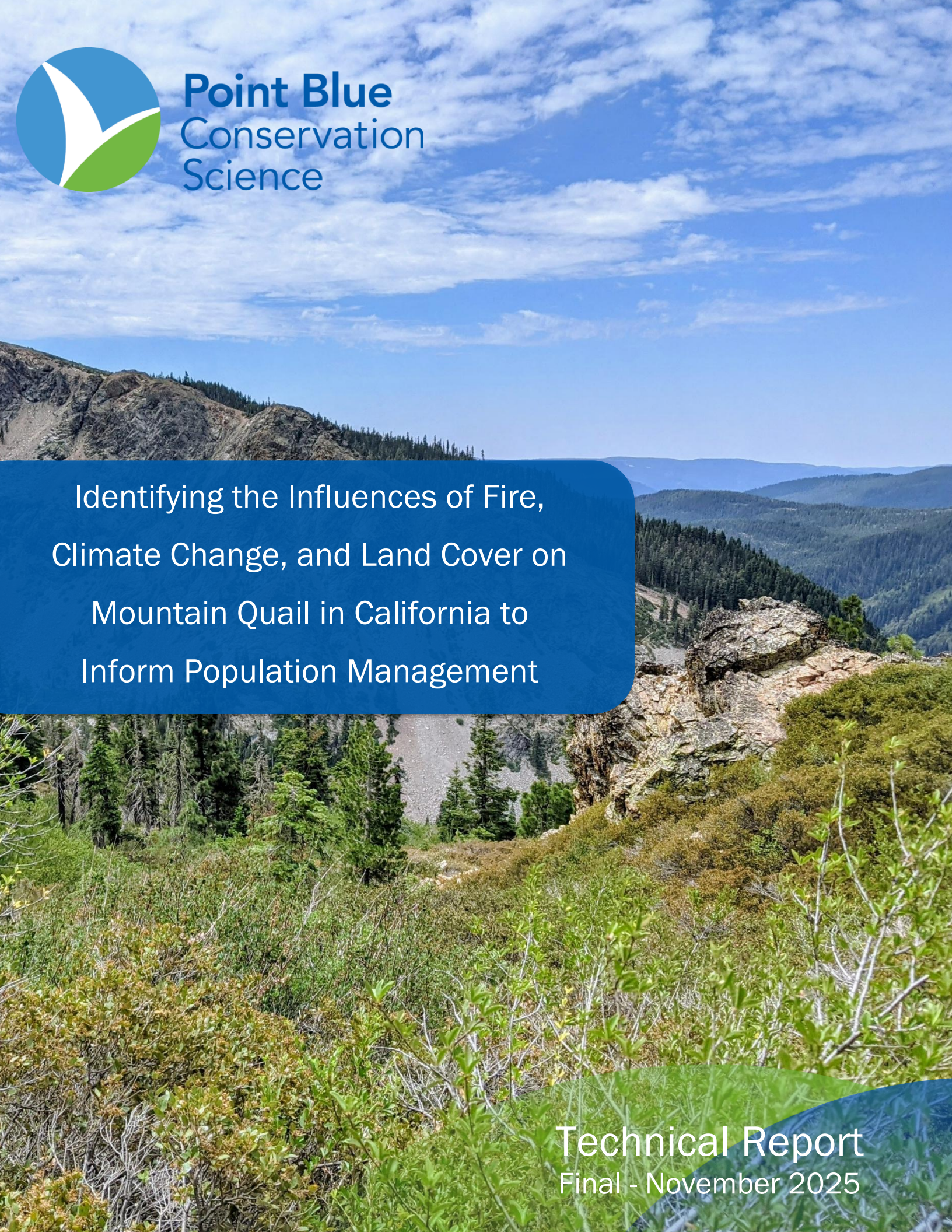

Point Blue Conservation Science

Identifying the Influences of Fire, Climate Change, and Land Cover on Mountain Quail in California to Inform Population Management

Technical Report

Final - November 2025

Photo description: Mountain Quail, Rob Fowler / Macaulay Library at the Cornell Lab (ML457742471)
Cover photo: Mountain Quail habitat in the Sierra Nevada, California. Photo credit: Brent Campos.

Identifying the Influences of Fire, Climate Change, and Land Cover on Mountain Quail in California to Inform Population Management

November 2025

Final report to the California Department of Fish and Wildlife in partial fulfillment of Grant Q2280166

Prepared by

Point Blue Conservation Science

Josée S. Rousseau, Brent Campos, Leonardo Salas, Ryan Burnett

With funding from

California Department of Fish and Wildlife (Grant Q2280166)
USDA Forest Service (Agreement 24 -CS-11052007-014)
The Marcia Grand Foundation

Suggested citation:
Rousseau, J.S.*, L. Salas, B. Campos, and R.D. Burnett. 2025. Identifying the influences of fire, climate change, and land cover on Mountain Quail in California to inform population management. Point Blue Conservation Science (Contribution No. 2567), Petaluma, CA.

*Corresponding author: jrousseau@pointblue.org

ACKNOWLEDGEMENTS

We would like to thank Katherine Miller, Dan Skalos, and Brett Furnas, from the California Department of Fish and Wildlife for their leadership and assistance with this project. Thank you to the numerous staff and volunteers who collected the field data and deployed recording equipment.

Mountain Quail habitat in the Sierra Nevada, California. Photo credit: Brent Campos.

ABSTRACT

Climate change and altered fire regimes are rapidly transforming montane forests of the Western United States and reshaping wildlife habitat, creating challenges for wildlife management. Reliable population monitoring is critical to inform management, yet it remains unclear whether emerging technologies like autonomous recording units (ARUs) provide information comparable to traditional point count survey methods by human observers when assessing the effects of fire, climate, and land cover, across multiple scales. We sought to better understand the effects of fire, climate, and land cover on Mountain Quail abundance and occurrence using point count and ARU data across the majority of their range in California and provide evidence-based recommendations for managing and monitoring this species in the context of dynamic environmental conditions.

We found that local-scale land cover best explained abundance, while landscape-scale land cover was more strongly linked to presence. In terms of land cover, the percentage of shrub cover emerged as important across all spatial scales (50-5,000 m). Fire-related factors were also broadly correlated with Mountain Quail presence and abundance with quail being positively associated with high burn severities 6-20 years post-fire at local scales (<500m) and positively associated with post-fire areas 1-5 years after fire if they burn heterogeneously at landscape scales. While climate variables were not strong predictors of abundance in isolation relative to land cover and fire, anomalously warm winter temperatures had a pronounced negative effect on abundance and presence in some regions. Abundance varied regionally with the highest population densities at lower latitudes. Population trends were consistently stable across regions and monitoring protocols from 2010 to 2021 in the Sierra Nevada, Southern Cascades, and Modoc Plateau, and in Northern California from 2017 to 2021.

Our findings suggest that while point counts and ARUs capture different aspects of Mountain Quail ecology, both provide complementary insights. We recommend that future monitoring continue with regional approaches, combine point counts with ARU data collection to strengthen inference and utility for management, and integrate multiple spatial scales during analysis.

TABLE OF CONTENTS

INTRODUCTION

Climate change is transforming the habitat of terrestrial wildlife in the mountains of the Western United States by reshaping and shifting the ranges of vegetation communities, altering hydrologic cycles, and amplifying thermal stressors (Halofsky and Peterson 2016, Thorne et al. 2018, Noel et al. 2025). Warmer winters, drier summers, and droughts have facilitated massive beetle outbreaks causing widespread mortality of conifer forests, which in turn affects wildlife (Bentz et al. 2010, Roberts et al. 2019a, Fettig et al. 2019, Madakumbura et al. 2020). Montane environments are experiencing reduced and earlier melt of snowpack, drying habitats that wildlife rely on (Wilkins et al. 2019, Halsch et al. 2024). Climate change also exerts direct thermal effects on wildlife, impacting survival and reproduction (Dugger et al. 2016, Riggio et al. 2023a). But perhaps nowhere are the effects of climate on wildlife habitat in Western montane forests more pronounced than those of increasing high severity fire.

California's forests, like much of the Western US, are experiencing rapid ecological change caused by altered fire regimes (Halofsky et al. 2020, Gaines et al. 2022). The fire regime across the majority of the conifer forest of interior Northern California and Sierra Nevada were historically characterized as mixed severity, dominated by lower and moderate severity effects, resulting in a structurally diverse and successionally heterogenous landscape (Hessburg et al. 2016). Following nearly a century of effective fire suppression, in the last few decades fires have been increasing in size and severity with a concomitant increase in the area burning at high severity and the size of the high severity patches, both outside the historic range of variability (Mallek et al. 2013, Steel et al. 2015, Hagmann et al. 2021, Williams et al. 2023). The abundance and distribution of forest successional stages has rapidly changed as a result, with homogenization of habitat patches at large landscape scales (Steel et al. 2023). These changes in turn affect the distribution and abundance of the wildlife communities adapted to the structural and spatial diversity created by mixed severity fires (Zeller et al. 2023).

Managing wildlife populations in these rapidly changing environmental conditions presents significant challenges for managers. Managers rely on the best available science to inform decisions, yet the pace of environmental change may lead to shifts in the species-habitat relationships that underpin decisions (Morley et al. 2018, Morelli et al. 2025). Recent technological advancements in wildlife monitoring, such as the use of autonomous recording units (ARUs), may help expand our capabilities to monitor wildlife populations (Dalton et al. 2022). ARUs present benefits for monitoring vocal wildlife such as birds (Darras et al. 2018). They offer a relatively low cost monitoring design, while typically increasing detection probabilities (Drake et al. 2021), especially for species with low detectability (Doser et al. 2021, Lewis et al. 2025). They have been shown to be effective in modeling habitat relationships for many bird species in the mountains of Northern California and the Sierra Nevada, including Mountain Quail (Furnas 2020, Brunk et al. 2023a, 2025). However, little is known about whether ARU and human observer assessments identify the same processes affecting wildlife, such as fire, climate, and land management.

The adoption of new monitoring methods can also present challenges for managers, especially for long-term monitoring programs. In some cases, the population estimates derived from new monitoring methods align with traditional monitoring methods, reinforcing their reliability (Baldwin et al. 2023, DeLeon et al. 2023). However, discrepancies in population estimates obtained from new and traditional monitoring tools (Hutto and Stutzman 2009, Hodgson et al. 2018, Drake et al. 2021, DeLeon et al. 2023) raise concerns for wildlife managers. Additionally, many of these technologies rely heavily on artificial intelligence (AI) models for data processing (Shah et al. 2020, Kahl et al. 2021, Vélez et al. 2023, Samiappan et al. 2024). It is important to compare trends in populations obtained from new technologies with traditional monitoring methods and identify the cause of discrepancies, if those exist (Strang et al. 2025). However, the type of data that feeds into population trends often differs across monitoring approaches. For example, point-count protocols are well suited for estimating abundance, whereas ARUs typically generate occupancy or presence/absence data (DeLeon et al. 2023). Depending on management goals, ARUs may not provide the data needed to guide management practices, especially in cases where accurate estimates of population size are required, such as for developing or adjusting hunting regulations. It is also important to evaluate if the covariate effects between traditional and new methodologies are comparable. Given the extent to which the existing literature on avian abundance and distribution is based on human observer counts, more comparisons of data collected by human observers and ARUs are needed as ARU data becomes more prevalent.

The Mountain Quail (*Oreortyx pictus*) is a small gallinaceous bird native to mountainous areas from Oregon, through California, to northern Baja California. They are associated with early and mid-successional stages of mixed conifer and mixed conifer-hardwood forests and shrublands (Block et al. 1987, Gutiérrez and Delehanty 2020). As an upland game bird and an indicator species for the US Forest Service, Mountain Quail is a species of high management interest in California, but few studies of the species exist to inform population management (Gutiérrez and Delehanty 2020), especially in relation to environmental change. In the Sierra Nevada, Mountain Quail have been found to respond positively to high-severity fire disturbances (Taillie et al. 2018, Brunk et al. 2023b) but these studies were limited in temporal or geographic scope. No published studies have evaluated Mountain Quail response to variations in climate in California, such as anomalous temperature and precipitation. In Idaho and Eastern Washington, they were found to be sensitive to climatic variables (Stephenson et al. 2011).

Our study sought to better understand the effects of fire, climate, and land cover on Mountain Quail abundance and occurrence across the majority of their range in California and provide evidence-based recommendations for managing and monitoring this species in the context of dynamic environmental conditions. We used data from long-term point count monitoring and recent ARU monitoring to model abundance and presence of Mountain Quail across the Sierra Nevada and Northern California mountains. By comparing results derived from these two monitoring techniques, we aimed to identify areas of agreement and discrepancy in the monitoring methods. We hypothesized that both methodologies (a traditional point count method and a new method using ARUs) would correlate broadly.

METHODS

Mountain Quail Detection Data

We used two types of data from three different sources to assess the breeding population trends and distribution of Mountain Quail across the majority of their range in California. The first data type consists of standardized point count surveys (Ralph et al. 1993) conducted across the Sierra Nevada Planning Area as part of a region-wide avian monitoring project on National Forest lands (Roberts et al. 2011b) (Figure 1). Sample locations were selected across nine National Forests and the Lake Tahoe Basin Management Unit using a generalized random-tessellation stratified design (GRTS) to avoid clustering in any given area. Within each GRTS area, surveys were located at elevations ranging from 1,000 to 2,800 meters, were limited to areas within 1 km of accessible roads, on slopes less than 35 degrees, and within forest, shrub wet meadow and riparian habitats. Sample locations formed a spatially balanced survey design with a geographically even distribution of sampling sites (Roberts et al. 2011a). The sampling design for upland habitats (forest and shrubland) included 2 transects per site, with each transect sampling a 1-km grid cell. Each upland transect consisted of 5 survey stations, a central station and four stations 250 meters away from the central station in each cardinal direction. The sampling design for wet meadow and riparian habitats included 2-3 transects per site with 4-5 stations arranged 250 meters apart in a linear or clustered pattern that sampled irregularly and linearly shaped habitat patches. Bird surveys were conducted from mid-May through early July from 2010 to 2021, except 2018 and 2020. Each survey consisted of a five-minute count, where the observer recorded the number and estimated exact distance to each individual bird species heard or seen, from the

Figure 1. The study area covers the Sierra Nevada mountain range, the northern California coast and northern mountain ranges. The dots represent the locations of the surveys from each data owner.

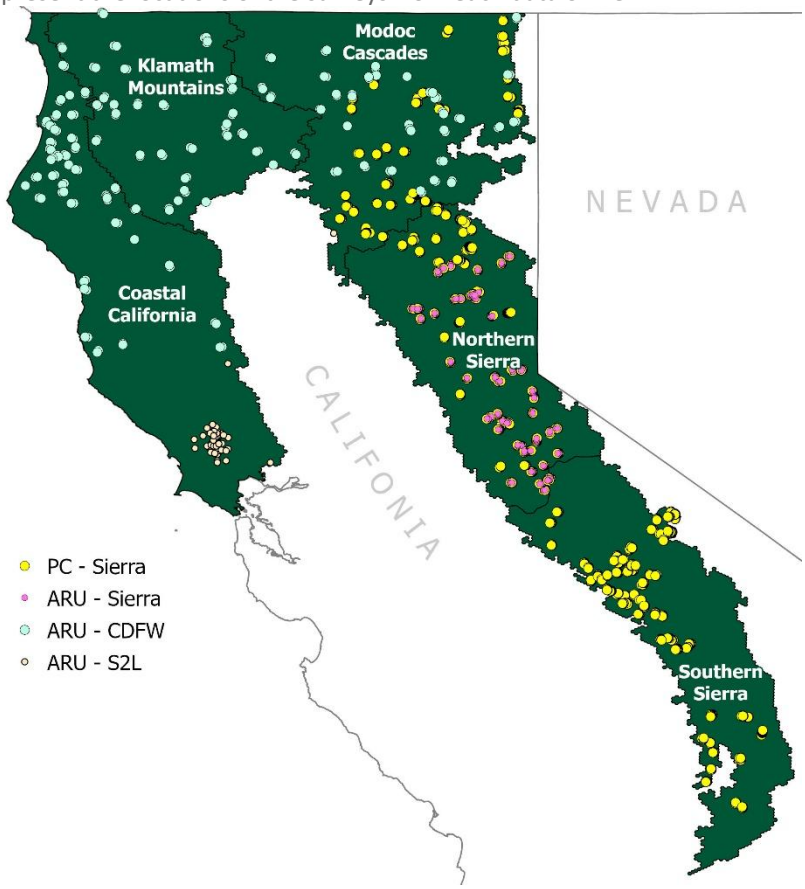

station center, out to a distance of 300 meters. Surveys began at local sunrise, were completed within four hours, and did not occur in conditions that would substantially reduce detectability (e.g. precipitation, fog, or high winds). Laser rangefinders were used to assist in distance estimation. While approximately 25% of all sites received a second visit every year, we used only observations from the first visit. We used a total of 15,781 point count surveys in the analysis.

The second data type came from Autonomous Recording Units (ARUs), deployed across the Northern California mountains and northern half of the Sierra Nevada (Figure 1;Furnas and Callas 2015, Snyder et al. 2022). All ARU data were recorded using Audiomoth devices (Hill et al. 2018, 2019). We used three sources of ARU data, each with their own recording protocol: Point Blue (Point Blue 2021), California Department of Fish and Wildlife (CDFW; (Furnas and Callas 2015), and Soundscape 2 Landscape (S2L; (Snyder et al. 2022). We used a sample (n = 1,737) of S2L recordings from Sonoma County, from April to June of years 2017 to 2020, only for tuning the convoluted neural network (CNN) model (i.e., not in the occupancy analysis; Snyder et al. 2022; details below). Data from CDFW consisted of 3 daily 5-minute recordings (n = 3,449) collected between pre-dawn (4:44 AM) and sunrise (6:33 AM) from May 2, 2017 to June 30, 2021, in the Northern California mountains (Figure 1). Recordings from Point Blue were sampled across the northern half of the Sierra Nevada in 2021 (Figure 1). They consisted of 1-minute recordings every 10 minutes of every hour for several days at each location. Because both the sampling design and sampling effort (number of years) differed between the CDFW and Point Blue, we opted to complete a separate occupancy analysis with each dataset. However, within a yearly scale, we subsetted the Point Blue dataset to the same months and approximate time periods of the CDFW dataset. That is, we used 15 minutes of recordings from each day, starting at 4:30 AM to 7:00 AM (n = 6,495 recordings). A total of 9,944 minutes of recorded data were used to predict with our tuned CNN model and resulted in 434,548 predictions of possible detections.

Cloud-based workflow to detect species using ARU recordings

We developed a cloud-based workflow that uses machine-learning techniques to accurately identify Mountain Quail vocalizations from ARU data. This system is scalable, allowing for future adaptations to include other species and regions. Beyond the immediate goal of identifying Mountain Quail, this workflow could be extended to increase the utility of the CDFW dataset for other species of management interest.

The cloud-based species detection workflow (Figure 2) included five steps: data labeling, data preparation, CNN model tuning, CNN model predictions, and CNN model evaluation. All of these steps were completed on a cloud computing system (the Amazon AWS cloud, or in the case of developing labels, the ARBIMON web platform). However, they could all be completed

on a local computer, provided that it has sufficient storage capacity. Below we describe each step and where it was completed.

Data labeling involved identifying the 'quark' song of Mountain Quail in a sample of recordings. This was completed using an automated detection tool in ARBIMON, a free web application (Aide et al. 2013). In ARBIMON, we searched for Mountain Quail 'quark' by listening to recordings and selected three templates of the call in a spectrogram. We then applied ARBIMONs image searching algorithm to find spectrograms in the same frequency range from our morning and afternoon recordings. Then, experts validated the detected 'quarks' as either 'present' or 'not present' (i.e., was or was not a Mountain Quail 'quark'), by inspecting all the findings of the pattern matching algorithm from ARBIMON. The results of the pattern matching searches and validations were exported out of ARBIMON as a csv file that contains: the name of the sound file, the starting and ending second where the pattern was located, and whether it was confirmed as a present or not present. Other software can be used to complete this task, including desktop applications, but these may lack an image or pattern searching tool and may require much more effort scanning large numbers of sound files to find matching patterns. We also note that the ARBIMON tool has an important caveat: the matches found are very similar to the pattern provided, thus there will be significant homogeneity in the results. It is always good practice to use several patterns to obtain some variability in the matches. We used three templates in our pattern matching analysis.

In the data preparation step, we used the downloaded csv file with the results of the pattern matchings to locate and crop the clips in the sound files. Because the next step requires 3-second clips and the patterns are usually shorter than 3 seconds, we centered and buffered the clips equally on both ends. We obtained over 7,000 tuning clips (both quail and non-quail detections combined). We ensured that these clips came from a variety of sample locations representative of the geographic diversity of our study area to enhance the diversity of the training patterns. We did not use any augmentation methods, which are commonly used to increase sample size, such as adding noise to our existing training clips to generate new tuning clips. This data preparation step can be completed on any platform with sufficient disk space to host the often-large sound files. Our AWS system consisted of an EC2 virtual machine with an Ubuntu 24.04 LTS operating system. On this machine we set up a Jupyter Notebook server, allowing us to access this computing environment from anywhere via a web URL connection. The server is password-protected. The sound files are stored in an Amazon S3 bucket, which we mounted onto the virtual machine and were thus available to the notebook server. We installed an R kernel for the notebook server, in addition to the default python kernel, to be able to run both python and R notebooks. Clipping the sound files with the pattern-matching results was done in R.

To predict quail presence in the recordings, we used the BirdNET CNN AI model. BirdNET is a freely available tool for identifying bird species from sound recordings across North America and beyond (Kahl et al. 2021, McGinn et al. 2023), and is accessible through its GitHub repository. The downloadable package includes a Python interface that allows users to both

train the model and run predictions on sound files. Following a transfer-learning approach, the code fine-tunes the classifier head of the CNN (i.e., the weights for the embeddings) without altering the original embeddings. For the tuning step, we used the 'autotune' functionality with 200 trials to optimize model hyperparameters (note that only a subset of CNN hyperparameters can be tuned using the provided software). We also used the 'append' functionality, which directed the model to use our numerous, geographically localized recordings of Mountain Quail. This step produced a classifier fine-tuned specifically on our data. To further improve accuracy, we included the provided "not-quail" clips so that the model could learn to distinguish quail vocalizations from similar sounds, thereby maximizing true detections while reducing false positives. Although BirdNET includes a Python application for training and prediction, we executed these steps from within R by calling Python scripts through system commands. For example, a batch execution of the BirdNET Python script from the command line might look like:

> python3 -m birdnet_analyzer.analyze … (other arguments here)

Then the R-based command would be:

$ system("python3 -m birdnet_analyzer.analyze … (other arguments here)")

The sole advantage of this approach is that it permits the user of our system to execute all steps within the R environment. Because we set up R to run in a Jupyter Notebook, users can fully annotate their code. We annotated all of our notebooks and documented every step described here.

The prediction step used the Mountain Quail classifier generated in the previous step to determine whether Mountain Quail were present in the recordings. Predictions were made on 1-minute or 5-minute recordings, with the model evaluating overlapping 3-second clips (1-second overlap). As with training, this was implemented as a batch script execution within the R environment, run in a Jupyter Notebook with an R kernel. Each prediction returned a confidence score indicating the model's certainty that a 3-second clip contained a Mountain Quail call. In addition to quail detections, we also applied the default BirdNET classifier to identify 20 additional species in the recordings. These consisted of the 10 most frequently and 10 least frequently detected species from point counts conducted at locations where Mountain Quail are known to occur (Appendix A).

Figure 2. Diagram of the workflow used to process and analyses the ARU data.

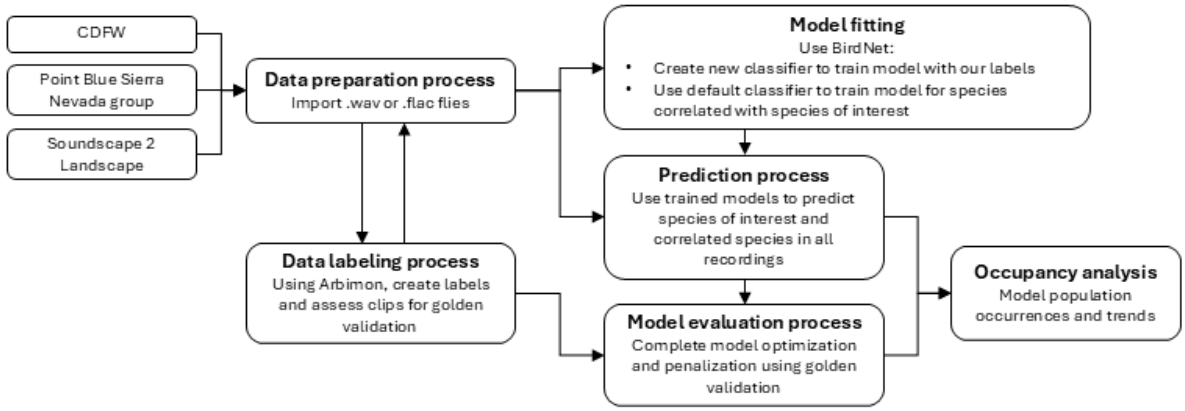

The final step, CNN model evaluation, focused on identifying the optimal level of prediction penalization to minimize false positives while maximizing true positives. Penalization can be applied simply by setting a minimum confidence threshold (e.g., accepting only predictions with confidence scores >0.8). This step is critical, as even a small number of false positives can significantly reduce accuracy (Royle and Link 2006, Miller et al. 2011, 2015, Royle et al. 2012). Because the CNN generates a confidence score for every 3-second clip, it is essential to determine the confidence level at which predictions can be considered reliable detections. Despite its importance, this step is often overlooked in similar studies, or a simple 0.5 threshold is used. To properly validate our model, we used a withheld dataset in which experts manually reviewed recordings. Reviewers documented the exact timing of Mountain Quail 'quark' calls, noted other detected species, and recorded background noise such as wind, insects, or human activity (Clark et al. 2023). We refer to this test set as our "golden validation" dataset.

To evaluate the performance of the AI model, we compared its predictions against the golden validation dataset. This allowed us to determine the confidence score threshold that balances prediction precision (accuracy) and recall (detection sensitivity). In a first step, we used the F_β index at $\beta = 1$ (highest recall) to identify a penalization threshold of 0.81, which yielded 75% recall and 87% precision. After identifying the penalization threshold, we found that the resulting detections still included a 13% false positive rate, so we took a second step of fitting an ensemble of Random Forest models, weighted and averaged across bootstrap replicates, that incorporated information from co-occurring species. This ensemble refinement provided a more reliable distinction between true and false positives and further improved overall precision. More details about the evaluation steps are provided in Appendix B.

Abundance and occupancy modeling analysis

Environmental covariates

We modeled Mountain Quail abundance and distribution using covariates relevant to the ecology of Mountain Quail with the inclusion of specific covariates to assess the impact of climate and fire. A total of 85 and 90 covariates were used in the modeling with the point count and ARU data, respectively. Each covariate consisted of a unique combination of measurement

(e.g., shrub cover, precipitation), spatial scale (e.g., 100m), and summary statistic (mean or standard deviation). See Appendix C for a complete list and definition of the covariates, their source, the spatial scales considered, and how they were summarized. The covariates fell in five broad data types: (1) survey effort, such as day of year and time of day; (2) geographic, such as latitude, aspect, relief, and an index of elevation; (3) climatic, related to annual temperature and precipitation anomalies; (4) landcover, such as satellite-derived metrics of land cover types, spectral wavelengths, and field-collected vegetation data; and (5) fire, such as the extent of high-severity fire, the number of years since the last fire, and a pyrodiversity index. Many of these covariates, particularly those related to land cover types and fire, were summarized across multiple spatial scales, ranging from 50 to 5,000 meters, and in some cases, across multiple ranges of years, e.g., high severity fires in the past one to five years. The 50 m covariates were obtained through field surveys, while all other scales – 100, 250, 500, 1,000, 2,000, and 5,000 m – were obtained using remotely sensed data. The original grain size of these remote sensing data was typically 30 m, beside the climate data which were provided at a 4,683 m resolution. These scales have been found to be relevant to avian ecology in other studies (Graf et al. 2005, Cunningham and Johnson 2006), while accurately representing land cover (Rigge et al. 2025).

Abundance analysis using point count data

We modeled the abundance of Mountain Quail over time in the Sierra Nevada and Modoc-Cascades regions using point count data (Figure 1). We used the 'distamp' function in the R package 'unmarked' (version 1.4.3; Kellner et al. 2023), a hierarchical modeling approach that models abundance corrected for detection as a function of distance from observers. Our models included all Mountain Quail detections up to a distance of 175 meters from each of the four cardinal point count stations of each transect. We excluded the central point count station at each transect to ensure no overlap in area sampled among adjacent point count stations at the 175-m distance threshold.

We applied a model selection process to account for imperfect detectability. We first compared three detection functions — hazard rate, half-normal, and uniform — via AIC with intercept-only formulas for the detection and abundance components of the models. We selected the hazard rate detection function for all subsequent analysis based on its lowest AIC value. We next assessed the influence of survey-specific variables on detection, evaluating the effects of Julian day, time of day, observer group, and habitat covariates on detection, while keeping the abundance formula as intercept-only. We compared candidate models using AIC and retained the top-performing model that included Julian day, time of day, and observer group. Lastly, for all abundance modeling, we considered counts from a station-year combination as independent records in the model, with year and transect as random effects to account for potential spatial and temporal patterns in abundance caused by repeated measures at the same locations (Fuller et al. 2016, Roberts et al. 2019b) and to account for yearly variation not represented by the covariates e.g., diseases, changes in phenology, etc. We also standardized all covariates prior to inclusion in the models by rescaling the data to have a mean of 0 and a standard deviation of 1. In the R analysis tool 'distsamp', we selected for the output to be the density in kilometer

square. We next used a model selection process to define the abundance formula in our models.

The environmental covariates that influence the abundance of Mountain Quail vary across their range (Rousseau and Betts 2022). We hypothesized that drivers of Mountain Quail abundance could differ across the broad geographic extent of our study area. To address this, we assessed the importance of environmental covariates in three geographic regions delineated using CDFW's ecoregion boundaries as a rough guide (Goudey et al. 2007): the Modoc-Cascades, the Northern Sierra Nevada, and Southern Sierra Nevada (Figure 1). We built separate models for each of these regions to assess varying geographical drivers and improve model fit (Syphard et al. 2024).

For each region, we developed four process models to evaluate the relative influence of climate, fire, local and landscape land cover on Mountain Quail abundance. These models aimed to identify which of these four ecological drivers were the most influential in predicting Mountain Quail abundance in each region. We used a two-step procedure to determine which covariates to include in each process model (steps 2 and 3 in Figure 3). In the first step, we combined all environmental covariates within each scale, to obtain one model per scale. For example, a scale model would have included vegetation covers, fire covariates, and so on, summarized at 100 m buffer. We also created one 'no scale' model for those covariates that were scale-independent (e.g., distance to river). At this step and all subsequent models we used the Variance Inflation Factor (VIF) to ensure no covariates within the same model had high correlation (VIF > 3) to avoid spurious model behavior (Akinwande et al. 2015, Yu et al. 2015). The second step involved selecting the covariates that would be included in each of the four process models for each region using the results of the spatial scale models. All climatic covariates were restricted to the climate model. All fire covariates were restricted to the fire model. All land cover covariates summarized at scale ≤ 500 m (buffer of 100 m, 250 m, and 500 m) were restricted to the local land cover model, while covariates summarized at scale ≥ 1000 m (buffer of 1000 m, 2000 m, and 5000 m) were restricted to the landscape land cover model. All four process models had the same detection formula as described above. Additionally, all models included the same subset of geographic variables and survey effort variables (Julian day) as fixed effects in the abundance formula (Appendix C). Some individual land cover and fire covariates were correlated across multiple spatial scales (e.g. shrub cover at 100m and 250m). To select the best scale for each covariate, we used the scale with the highest absolute z-value (mean estimate divided by standard error) from the previous step. The final set of covariates for each process model in each region is listed in Appendix D. Finally, we compared the four process models within each region using AIC to determine which process best explained the variation in Mountain Quail abundance. This process model comparison was completed for the two Sierra regions but was not for the Modoc-Cascades region due to a lack of convergence for some of the process models.

Next, we developed a final model per region for assessing population trends and predicting the species' distribution. For the two Sierra Nevada regions, we first ran a global model per region containing all covariates present in at least one of the process models (Figure 3; Appendix D).

We then reduced the number of covariates in the model by removing any that had a p-value > 0.1. This step sometimes included iterations of running models. We then further reduced the covariates by removing any with a p-value > 0.05, again running model iterations until all covariates had a p-value < 0.05. We observed that some iterations sometimes had a lower AIC even if it contained covariates with a p-value > 0.05. If such was the case, we kept the model with the lowest AIC (retained the covariate). For the Modoc-Cascades region, we used a univariate approach to build the final model, where we selected all covariates significantly correlated with abundance, starting with the one with the largest effect size, and sequentially added covariates until the model no longer converged because of sample size limitations. We then compared a few candidate models using AIC and selected the best-fit model. For the final models for all regions, we assessed if we had spatial autocorrelation in the residuals using Moran's I (Fortin et al. 1989, Betts et al. 2006), as the presence of spatial autocorrelation can affect model fit (Betts et al. 2006, Bahn et al. 2006). Although Moran's I values were statistically significant, they remained low (< 0.1) and only within very short distances (not among transects), indicating minimal positive spatial autocorrelation (Appendix E). Finally, we assessed model fit for each region's final model using a goodness-of-fit test (parboot function, 100 simulations; Fiske and Chandler 2011).

We assessed trends in Mountain Quail population density in each region from 2010 to 2021. First, we predicted the population density of each year of sampling using each region's final model. We then fit a linear regression model to these annual density predictions to assess the population trend.

Figure 3. Summary of the methodology used to predict abundance from the point count data and presence from the ARU data.

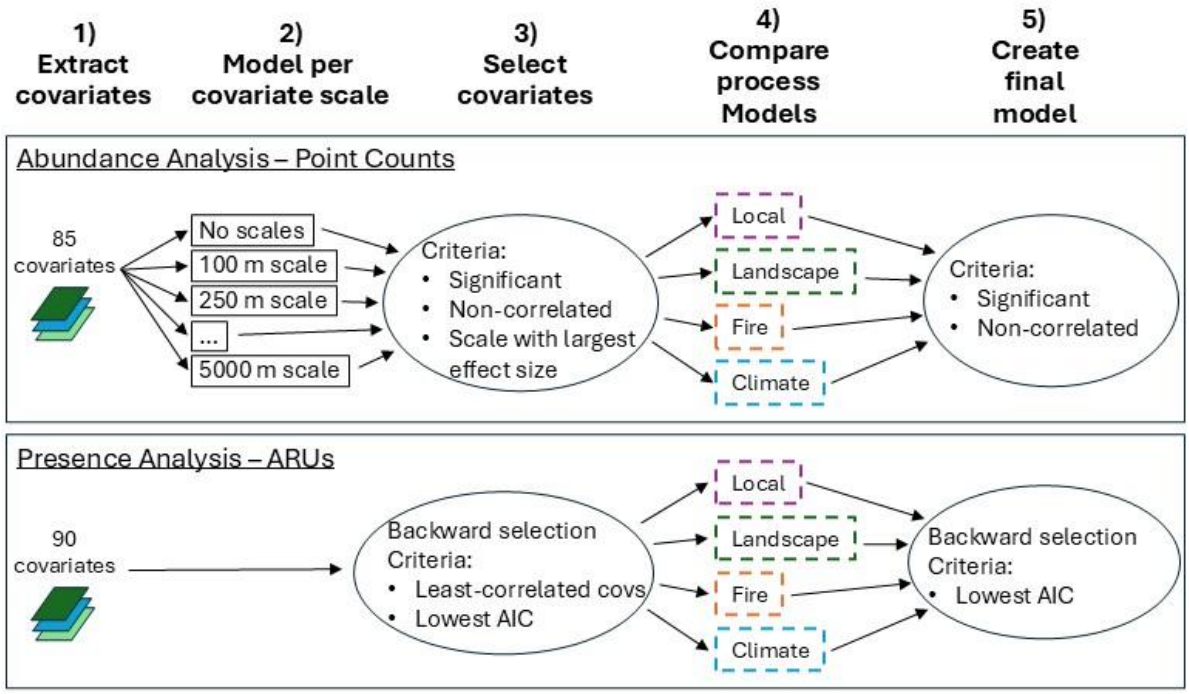

We created a map of the predicted abundance of Mountain Quail using the final model for each region. We predicted density at the central point of a 2.5 square mile hexagon grid used by the CDFW Areas of Conservation Emphasis, using remotely sensed covariates values for 2021. However, the final model of each region included a field measurement, shrub cover, not available across the hexagon grid. We thus used the regional mean of shrub cover in our prediction calculations. While not perfect, this allowed us to visualize the variation in abundance as a function of all the other covariates in the model. The mapped predictions were constrained to hexagons with values of covariates within the range of our samples for each regional model.

Presence-absence analysis using ARU data

We used a similar approach to assess the presence and absence of Mountain Quail using ARU data as we employed for the abundance analysis, with some noteworthy differences (Figure 3). We used two regions for this analysis, the Northern Sierra and a Northern California region that was a combination of the Coastal California, Klamath Mountains, and Modoc-Cascades regions (Figure 1). The Northern Sierra Region contained Point Blue ARU data from 2021 that overlapped with point counts at the same sample locations. The Northern California region contained CDFW ARU data collected from 2017 to 2021. We created this larger region to increase sample size for analysis.

All Mountain Quail detections were obtained from the CNN model predictions after the penalization and correction process (the CNN model evaluation process). For each region, we summarized acoustic detections by survey event, where an event was defined as 15 minutes of surveys at a site on a given date. This yielded six consecutive survey events (six consecutive days) per site-year. A survey event was considered to have a detection if at least one corrected positive detection occurred within the 15-minute period. We excluded 11 site-years from the Point Blue data that had fewer than 15 minutes of sound records.

We further noted that there was a clear dichotomy in the number of detections per survey event among sites. Specifically, we constructed the empirical probability distribution of all corrected detections from all 15-minute events across all site-years in the region, and sought to classify an event as having quail if the number of corrected detections exceeded some percentile of that distribution. For example, the 30th percentile of the distribution might be 3 detections per event, so any event with more than 3 detections would be considered as having detected the species, and not having detected the species if the number of detections in the event was 3 or fewer. Since each site has 6 survey events, we could construct a detection table where each row is a site and each column represents a single survey event and use this detection table to fit an imperfect-detection occupancy model. However, upon reviewing the data, a clear dichotomy was seen in the empirical distribution as it applied to survey site-years before applying any quantile filtering: most site-years with detections had 4-6 events with detections, while the rest of site-years had only 0–2 detections across all events. Given this pattern, we chose not to fit an imperfect detection model, and instead applied a logistic model. Thus, we coded a site-year as 1 (quail present) if it had 4-6 events with detections, and 0 (quail absent) otherwise. Doser et al. (Doser et al. 2021) noted in a simulation analysis that when

fitting hierarchical imperfect-detection models that include estimation of false positives to data from highly abundant species, the models failed to converge due to lack of parameter identification and thus inability to distinguish true from false positives. Our data were already corrected with an ensemble of Random Forest models to remove false positives, thus fitting a model with a false positive probability was unwarranted. We acknowledge that quail might have been present at sites with ≤2 detections, but this threshold also serves as an additional filter against false positives and may help address the problem noted by Doser et al. (2021) in high abundance areas. To account for seasonal variation in calling behavior, we included both linear and quadratic terms for day of year in the logistic model.

We created four process models, representing fire, climate, local land cover and landscape land cover as described above, one set for each region. In this case, covariates that were correlated were kept as long as they increased model fit based on AIC (Burnham and Anderson 2004). The selection of covariates in each process model was done using a backward stepwise algorithm. When using logistic models, it is recommended to balance the number of zeros and ones as the response variable (Salas-Eljatib et al. 2018). However, the Northern California region contained 6 times more ones than zeros. We thus repeated the process of creating the four process models 100 times, each using a bootstrap sample containing the same number of zeros and ones. We compared the process model using AIC to assess which process was most correlated with the presence-absence of Mountain Quail in each region.

For each region, we considered all covariates present in at least one of the four process models for inclusion in the final model and used the same backward stepwise algorithm to determine the covariates to retain. For the Northern California region, we thus obtained one final model per bootstrap. We assessed the goodness of fit of all 100 final models using a Hosmer-Lemeshow test (Hosmer and Lemesbow 1980, Hosmer et al. 1997).

We investigated for any temporal variation in presence in the Northern California region, where multiple years of CDFW's ARU data existed. We fit the best model possible with year as a categorical fixed effect. Because of the low number of ARU deployed and thus paucity of data in 2019 and 2020, we lumped these years with 2021, resulting in 3 year-classes with 23 data points for 2017, 45 for 2018, and 46 for 2019-21. We then assessed how many times the year effect was selected as a competitive covariate across the 100 bootstrapped iterations of the final model. We also created a partial dependence plot (PDP) for the year covariate, to inform if a trend was present.

We created a prediction map of the probability of presence across both regions using the final models. For the Northern California region, we used the mean prediction from each of the 100 bootstrapped models, inversely weighted by their AIC values.

Comparison between abundance and presence results

We compared predictions of abundance and presence in the two regions where both point count and ARU data were collected: the Northern Sierra and the Modoc-Cascades.

In the Northern Sierra, point count and ARU datasets were collected along the same transects, allowing us to compare predictions directly at survey points as well as across the entire region. For point-level comparisons, we used predictions on the original (untransformed) scale, while for regional comparisons we used back-transformed predictions. In the Modoc-Cascades, the point count and ARU datasets were collected at different locations. As a result, we restricted comparisons to regional predictions, again using back-transformed values. In both cases, we fit linear models to assess whether the two prediction types - abundance and presence - were correlated.

For the Northern Sierra, we further examined where and when abundance and presence predictions aligned and where they diverged. To do this, we scaled abundance values from 0 to 1 and subtracted the predicted probability of presence from the scaled abundance. Values near zero indicated strong agreement between models, negative values indicated higher predicted presence relative to scaled abundance, and positive values indicated the reverse. We then tested whether these differences were associated with particular covariates by fitting separate linear models for each covariate selected in either model.

RESULTS

Processes influencing abundance and occupancy

We evaluated if the Mountain Quail abundance and presence were most influenced by climate, fire, local or landscape land cover types. We found that the process influencing the abundance and presence differed across regions and data type. Overall, abundance tended to be better explained by local scale covariates, while presence patterns tended to be better explained by landscape scale covariates. The fire covariates formed a competitive model using the Southern Sierra abundance data and the Northern California presence data (Table 1; Appendix D).

Covariates correlated with abundance and presence

The covariates from the process models were used to create one final model for each region and data type (i.e., point count and ARU), resulting in five final models: Southern Sierra, Northern Sierra, and Modoc-Cascades for the abundance analysis, and Northern Sierra and Northern California for the presence analysis. Each of the five models achieved satisfactory goodness-of-fit results. For the abundance models, the parametric bootstrap of the sum of squared errors (SSE) showed that the observed statistic (calculated from the data and fitted models) had p-values of 0.373 for the Southern Sierra, 0.430 for the Northern Sierra, and 0.545 for the Modoc-Cascades region within the empirical distribution sampled from the posterior values of the predictors, indicating a sufficiently good fit.

For the presence analysis, the Hosmer–Lemeshow goodness-of-fit Chi-square test statistic for the Northern Sierra was 1.39 with 8 d.f., and a p-value of 0.99, demonstrating a good fit. For the Northern California region, the test statistic averaged 12.2 with 9 d.f., and mean p-value of 0.47 among all 100 ensemble models, also indicating an overall good fit, though 17 of the models did not have a good fit.

Table 1. AIC comparison of four process models for four regions. Models in bold, for each region, had substantial support (delta < 2).

Region*	Process Model	K	Log link	AICc	Delta	Weight
Northern Sierra - Abundance	**Local Land Cover**	**40**	**-5299.40**	**10679.29**	**0**	**1**
	Landscape Land Cover	26	-5348.27	10748.74	69.46	0
	Fire	28	-5353.05	10762.34	83.06	0
	Climate	22	-5365.34	10774.83	95.54	0
Southern Sierra - Abundance	**Fire**	**24**	**-4544.20**	**9136.64**	**0**	**0.63**
	Local Land Cover	**34**	**-4534.61**	**9137.70**	**1.05**	**0.37**
	Landscape Land Cover	31	-4541.98	9146.37	9.72	0
	Climate	23	-4556.49	9159.19	22.55	0
Northern Sierra - Presence	**Landscape Land Cover**	**20**	**-24.07**	**99.34**	**0**	**0.62**
	Local Land Cover	**23**	**-19.50**	**100.34**	**1.00**	**0.37**
	Fire	6	-47.92	108.78	9.44	0.01
	Climate	7	-48.94	113.14	13.81	0
Northern California - Presence**	**Landscape Land Cover**			**74.41**	**0**	**0.40**
	Local Land Cover			**74.75**	**0.35**	**0.34**
	Fire			**75.78**	**1.38**	**0.20**
	Climate			78.20	3.79	0.06

* This analysis was not completed for the Modoc-Cascades abundance.
** Results are the average AICc of 100 bootstraps.

Of the 85 covariates considered in the abundance analysis, and 90 in the presence analysis, 22 and 20 respectively were selected by at least one regional final model (Table 2). For the abundance analysis, two of the 22 covariates were selected in all three regional final models - day of year and field measured shrub cover within 50 m - 7 were selected by two regional final models, and 13 were unique to one regional final model (Table 2). For the presence analysis, only one of the 20 selected covariates were common to both regional final models - day of year - and 19 unique to only one regional model (Table 2). Covariates for near-infrared or red band reflectance values were present for all five regional models at scales ranging 100-1000 m (Table 2). Lastly, three covariates - the Landsat mean red band reflectance, summarized over a 100m, the mean percent tree cover, summarized over 5,000m, and the minimum winter temperature anomaly - were selected by at least one abundance and one presence regional model (Table 2).

While different covariates were selected in the abundance and presence regional models, those selected often measured similar features or the same features at different scales. For example, in the Northern Sierra region, Mountain Quail abundance was correlated with shrub cover within 50 m and 250 m, whereas the probability of presence was also correlated with shrub cover at broader scales of 2,000 m and 5,000 m (Table 2, Figures 4A-B).

Table 2. List of covariates correlated with Mountain Quail in each region. The models associated with the first three regions are abundance, while the last two are from presence models. The linear model (L) and quadratic (Q) model results include the estimate ± SE and the significance level – *** for p-values <= 0.001, ** for p-values <= 0.01, * for p-values <= 0.05, and . for p-values between 0.05 and 0.1.

			Point Count Abundance Analysis			ARU Presence Analysis	
Process	**Covariate**	**Scale**	**Southern Sierra**	**Northern Sierra**	**Modoc-Cascades**	**Northern Sierra**	**Northern California**
All	Average temperature	Yearly		L: -0.409 +/- 0.079 ***	L: 0.492 +/- 0.156 **		
All	Day of year	Daily	L: 0.140 +/- 0.315 Q: -0.218 +/- 0.077 **	L: -0.273 +/- 0.058 ***	L: -0.691 +/- 0.147 ***	L: -1.809 +/- 0.804 * Q: 2.000 +/- 1.038 .	L: -4.342 +/- 1.010 *** Q: -2.642 +/- 0.674 ***
All	Latitude	At point		L: -0.338 +/- 0.061 ***			
Local Land Cover	Aspect east-west slopes	100m		L: -0.194 +/- 0.043 *** Q: -0.105 +/- 0.041 **			
Local Land Cover	Aspect north-south slopes, mean	100m	L: 0.047 +/- 0.045 Q: -0.073 +/- 0.044				
Local Land Cover	Landsat near-infrared band, mean	100m	L: 0.148 +/- 0.047 **	L: 0.133 +/- 0.051 **			
Local Land Cover	Landsat near-infrared band, mean	500m					L: -2.054 +/- 0.897 .
Local Land Cover	Landsat near-infrared band, SD	100m				L: 3.654 +/- 1.567 * Q: -1.906 +/- 0.734 **	
Local Land Cover	Landsat near-infrared band, SD	500m			L: 0.160 +/- 0.101		
Local Land Cover	Landsat red band, mean	100m		L: 0.238 +/- 0.058 *** Q: -0.106 +/- 0.028 ***	L: 0.262 +/- 0.140 . Q: -0.420 +/- 0.110 ***	L: 1.340 +/- 1.517 Q: -3.252 +/- 1.258 **	
Local Land Cover	Percent shrub cover	50m	L: 0.120 +/- 0.039 **	L: 0.247 +/- 0.052 *** Q: -0.057 +/- 0.027 *	L: 0.257 +/- 0.069 ***		
Local Land Cover	Percent shrub cover, mean	250m		L: 0.278 +/- 0.074 *** Q: -0.087 +/- 0.030 **			
Local Land Cover	Percent tree cover, SD	500m		L: -0.096 +/- 0.059 Q: -0.135 +/- 0.038 ***	L: 0.283 +/- 0.117 *		
Local Land Cover	Shrub height, mean	100m					L: -1.043 +/- 0.652
Local Land Cover	Topographic relief	500m	L: 0.207 +/- 0.079 ** Q: -0.103 +/- 0.039 **				
Local Land Cover	Topographic relief	100m				L: 4.764 +/- 1.702 ** Q: -2.904 +/- 1.413 *	
Landscape Land Cover	Landsat near-infrared band, mean	1000m		L: 0.137 +/- 0.063 *			
Landscape Land Cover	Landsat near-infrared band, SD	1000m				L: 2.261 +/- 1.262 .	
Landscape Land Cover	Percent shrub cover, mean	2000m					L: 3.069 +/- 1.513 .

			Point Count Abundance Analysis			ARU Presence Analysis	
Process	**Covariate**	**Scale**	**Southern Sierra**	**Northern Sierra**	**Modoc-Cascades**	**Northern Sierra**	**Northern California**
Landscape Land Cover	Percent shrub cover, mean	5000m				L: 6.972 +/- 2.877 * Q: -5.312 +/- 1.690 **	
Landscape Land Cover	Percent shrub cover, SD	1000m				L: -11.157 +/- 4.236 **	
Landscape Land Cover	Percent shrub cover, SD	2000m				L: 5.313 +/- 3.036 . Q: 2.300 +/- 1.192 .	
Landscape Land Cover	Percent tree cover, mean	2000m				L: -9.684 +/- 4.200 *	
Landscape Land Cover	Percent tree cover, mean	5000m			L: -0.155 +/- 0.116	L: 5.734 +/- 2.834 *	
Landscape Land Cover	Percent tree cover, SD	1000m				L: -2.799 +/- 1.470 .	
Landscape Land Cover	Percent tree cover, SD	5000m			L: -0.364 +/- 0.108 ***		
Landscape Land Cover	Shrub height, mean	1000m				L: 6.493 +/- 3.171 *	
Landscape Land Cover	Shrub height, mean	2000m					L: -1.900 +/- 1.090
Landscape Land Cover	Topographic relief	2000m	L: 0.181 +/- 0.079 *				
Fire	Percent high burn fire severity	Past 1 to 5 yrs - 100m				L: -2.466 +/- 1.028 *	
Fire	Percent high burn fire severity	Past 11 to 20 yrs - 250m	L: 0.027 +/- 0.016 .				
Fire	Pyrodiversity index	Past 1 to 5 yrs - 1000m	L: -0.197 +/- 0.140 Q: 0.112 +/- 0.041 **	L: 0.365 +/- 0.151 * Q: -0.079 +/- 0.043 .			
Fire	Pyrodiversity index	Past 6 to 10 yrs - 100m	L: 0.314 +/- 0.120 ** Q: -0.057 +/- 0.020 **	L: 0.317 +/- 0.133 * Q: -0.063 +/- 0.024 **			
Climate	Maximum summer temperature anomaly	Current year	L: 0.227 +/- 0.079 **				
Climate	Maximum summer temperature anomaly	Past year					L: -2.773 +/- 1.169 *
Climate	Minimum winter temperature anomaly	Current year	L: -0.319 +/- 0.122 **	L: 0.147 +/- 0.109 Q: 0.147 +/- 0.056 **			
Climate	Minimum winter temperature anomaly	Past year	L: -0.429 +/- 0.121 ***				L: 0.152 +/- 0.874 Q: 1.984 +/- 1.034 .
Climate	Winter precipitation anomaly	Past year					L: -1.652 +/- 0.980 Q: 1.680 +/- 0.701 *

Metrics of vegetation structure appeared in the final model for every region. For all regions, Mountain Quail abundance or presence was associated with moderate to high shrub cover, with abundance peaking at 50-100% shrub cover at local scales and 10-50% shrub cover at landscape scales (Table 2). Tree cover metrics appeared in top models for all regions except Northern California, always at scales ≥ 500 m, and relationships varied across scales and regions (Table 2).

Fire covariates were retrained in the final abundance and presence models for the Sierra Nevada but not for the Modoc-Cascades and Northern California (Table 2). Several fire covariates caused a lack of model convergence and had to be removed. Mountain Quail abundance was positively associated with moderate pyrodiversity at 6-10 years post fire within 100 m of surveys in both the Northern and Southern Sierra (Table 2, Appendix F). In the Southern Sierra, abundance was also positively correlated with increasing proportion of high burn severity at 11-20 years post-fire at the 250 m scale (Table 2, Appendix F). Mountain Quail abundance was associated with moderate and high pyrodiversity for fires 1-5 years old at the 1000 m scale in the Northern and Southern Sierra respectively (Table 2, Appendix F). The only fire covariate associated with presence was a negative association with proportion of high severity burn 1-5 years post-fire within 100 m in the Northern Sierra (Table 2, Appendix F).

Climate covariates were retained in the final models for the Sierra Nevada and the Northern California regions. In the Southern Sierra Nevada, Mountain Quail abundance was negatively associated with anomalously warm winters (Table 2, Appendix F). Quail were predicted to be about three times as abundant in areas that experienced a winter 3℃ cooler than average than areas experiencing a winter 3℃ warmer than average (Appendix F). This effect carried over to the next breeding season, and was slightly stronger (Table 2, Appendix F), such that Mountain Quail populations were suppressed for two years in areas experiencing anomalously warm winter temperatures and vice versa for cold winters. The relationship with anomalous winter temperatures flipped in the Northern Sierra where Mountain Quail were predicted to be about five times more abundant in areas that experienced a 5℃ warmer than average winter compared to an average or slightly cooler than normal winter. Mountain Quail in the Southern Sierra were also positively correlated with anomalously warm summers (Appendix F). In the Northern California region, Mountain Quail presence was reduced in areas that experienced anomalously hot summer temperatures the year prior (Table 2, Appendix F). Though covariates for winter temperature and precipitation anomalies appeared in the final presence model for Northern California (Table 2), the relationships did not appear ecologically meaningful when plotted (Appendix F).

Figure 4. Selected partial dependence plots showing relationships between Mountain Quail abundance (plots A, C, and E) or presence (plots B, D, and F) and model covariates. A) Positive association between abundance and mid-range values of shrub cover within 50 m (field measurement), in the Northern Sierra. B) Positive association between presence and mid-range shrub cover summarized within a 2000 m buffer (remotely sensed), in the Northern Sierra. C) Positive effect of low pyrodiversity within 100 m on abundance, especially when fires occurred 6–10 years prior, in the Northern Sierra. D) Positive association between presence and a low percentage of the 100 m buffer that experienced high-severity fire within the past 1–5 years, in the Northern Sierra. E) Positive association between abundance and maximum summer temperature anomalies during the current summer, in the Southern Sierra. F) Negative association between presence and maximum summer temperature anomalies during the previous summer, in Northern California.

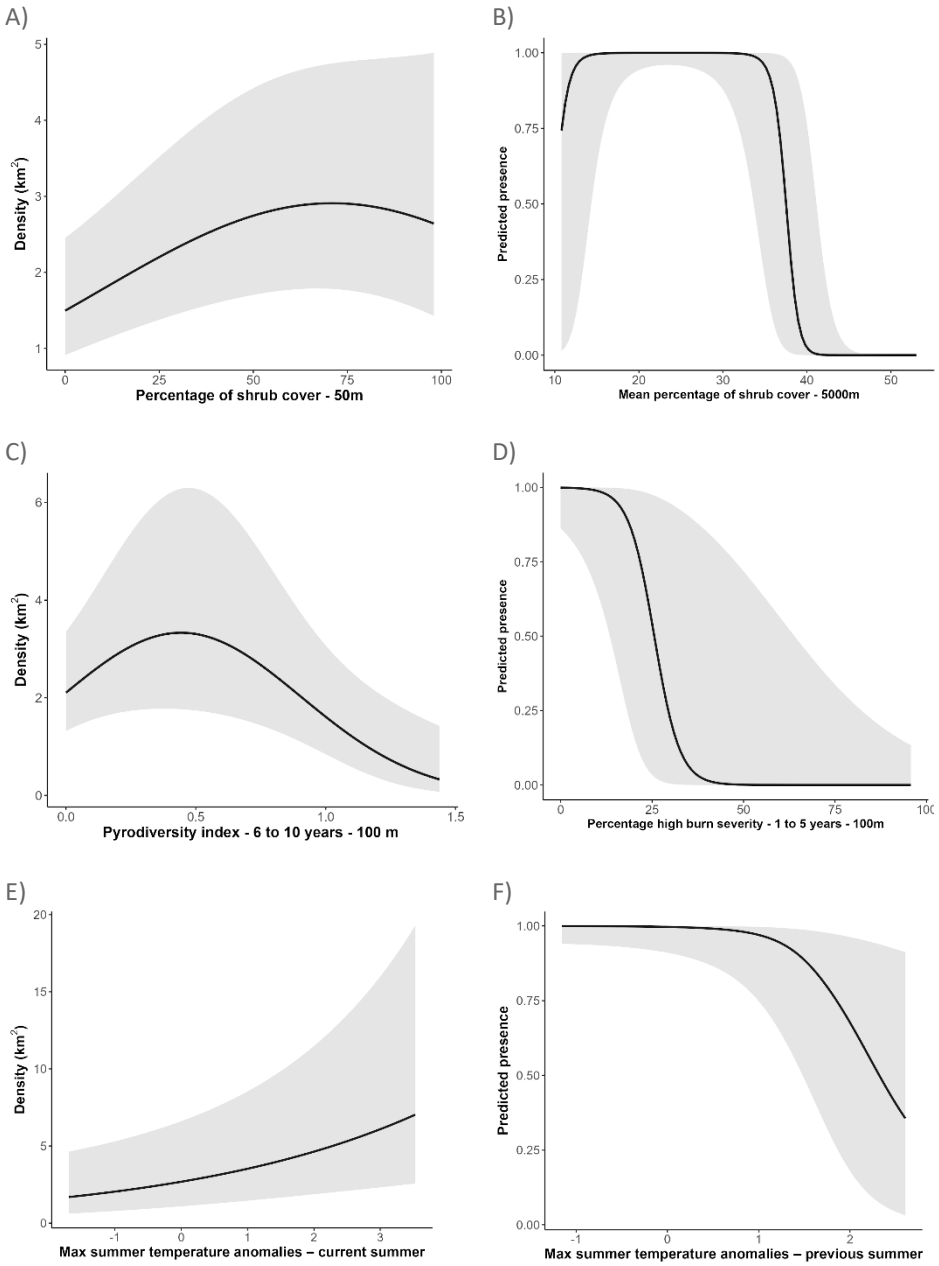

Predicted abundance versus presence

We compared predictions of abundance and presence of Mountain Quail across regions (Figure 5). The abundance and presence predictions for the Northern Sierra were positively correlated for both the survey locations and across the whole region ($F_{(1,90)} = 4.11$, $p = 0.04$; $F_{(1,2192)} = 16.17$, $p < 0.001$, respectively). However, the r-squares were very low (0.03 and 0.01, respectively), suggesting the correlations were not very meaningful. The predictions across the Modoc-Cascades region were significantly negatively correlated ($F_{(1,7794)} = 69.35$, $p < 0.001$), with a slope of -0.031.

In the Northern Sierra, abundance and presence predictions differed most when surveys occurred early or late in the season. Whether ARU and point count surveys were conducted at the same time or not made no difference. In other words, abundance and presence aligned only when both surveys were conducted mid-season. Moreover, survey dates for both data types were highly correlated with elevation, with low-elevation sites typically surveyed earlier in the season and high-elevation sites surveyed later, reflecting limited access due to snowpack.

Figure 5. Predicted A) presence and B) abundance across regions occupied by the Mountain Quail in the year 2021. We only predicted at locations within the range of covariates used to create the models.

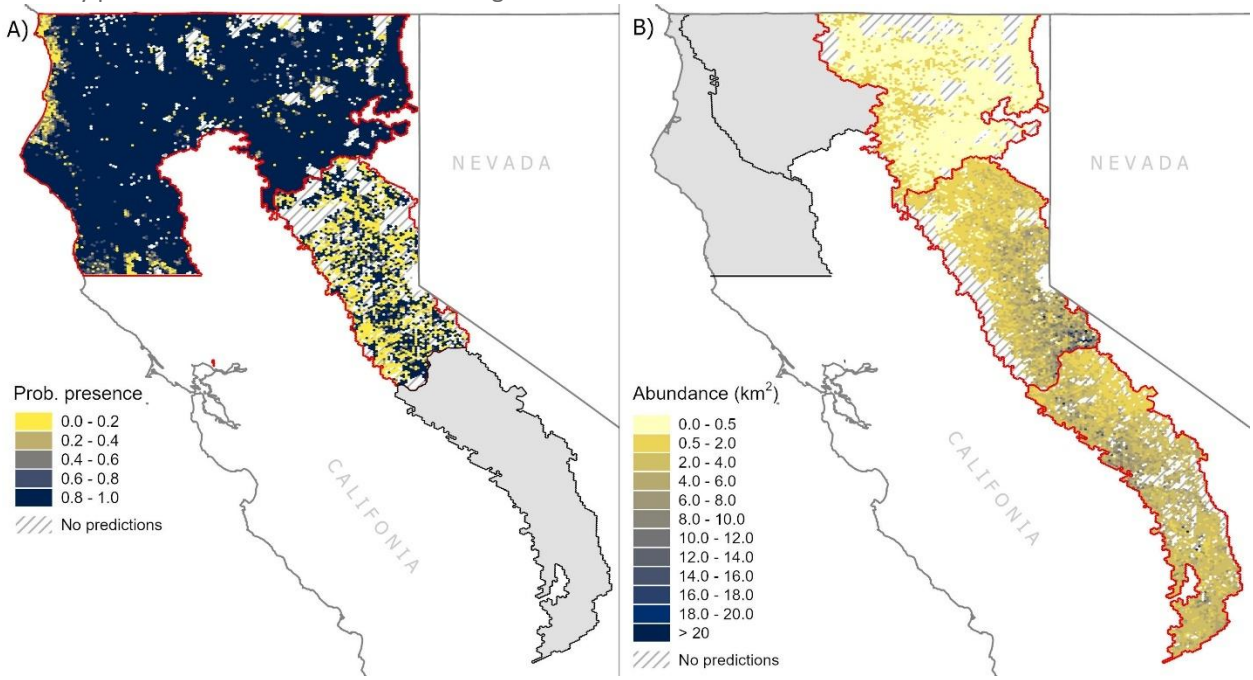

Trends in Mountain Quail Density

Mountain Quail population density varied among regions, but temporal trends were not apparent. Although Mountain Quail population density varied over time, especially in the Southern Sierra, trends from 2010 to 2021 appeared stable in all three abundance regions (Figure 6; Modoc-Cascades: slope = 0.037 ± 0.045, p-value = 0.434; Northern Sierra: slope = 0.025 ± 0.051, p-value = 0.644; Southern Sierra: slope = -0.006 ± 0.065, p-value = 0.935). Mean population density decreased with increasing latitude, from 3.5 ± SD 0.6 individuals/km² in the

Southern Sierra, 2.3 ± SD 0.5 individuals/km² in the Northern Sierra, to 1.0 ± SD 0.5 individuals/km² in the Modoc-Cascades (Figure 6).

Figure 6. Trend and mean density of Mountain Quail per region. All trends were non-significant.

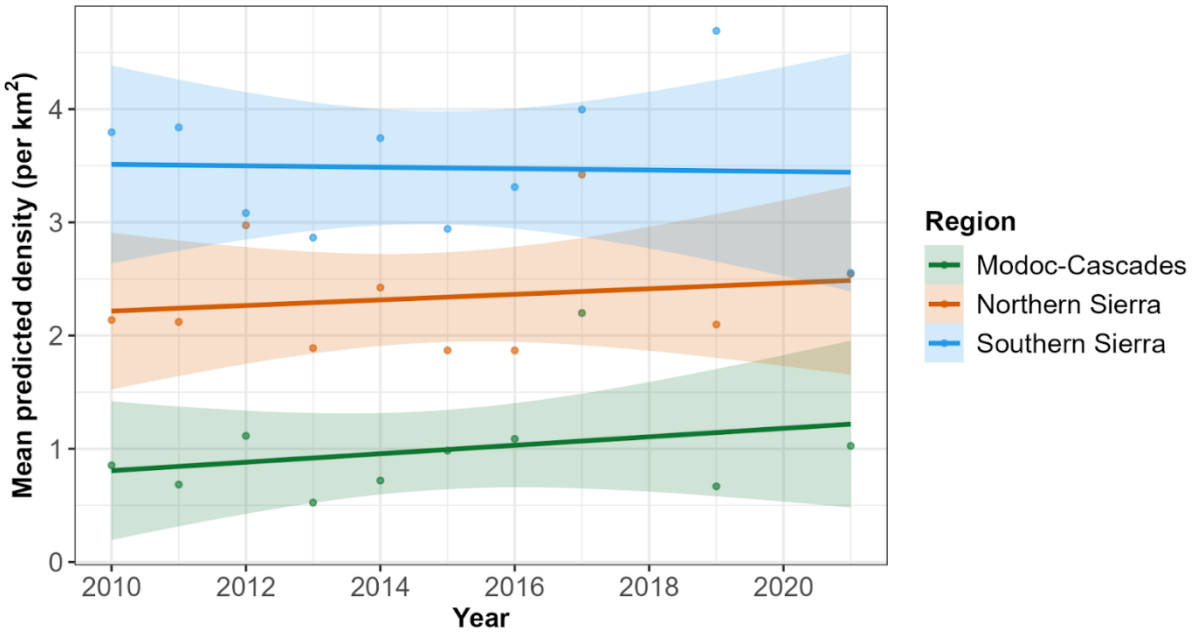

Using the ARU data, we were only able to assess trends in Mountain Quail presence in the Northern California region, since it was the only area with multiple years of data. We found no supporting evidence in the data for variation in the probability of quail presence among years. A model with fixed year effects required more parameters to be marginally competitive. Across 100 bootstrapped models for this region, year was retained as a final covariate in just 19 models, and predicted presence did not vary significantly across years (slope = 0.008 ± SE 0.008, t = 1.028, p = 0.491).

DISCUSSION

We assessed the impact of fire, climate, local and landscape land cover types on the abundance and presence of Mountain Quail with point count and ARU data in the mountainous regions of Northern California and the Sierra Nevada, California. Our results suggest that Mountain Quail abundance and presence was mainly correlated with land cover at local- and landscape-scales (out to 5000 m) that, at least in some regions, were shaped by fire processes. There were also smaller but concerning effects of temperature anomalies suggesting Mountain Quail may be susceptible to warming winters and summers in parts of their range. We did not find evidence of an ecologically meaningful effect of precipitation anomalies on Mountain Quail populations. While there was large annual variation in abundance in some regions, we found no evidence for a temporal trend in abundance or presence across the time scales in our study. Lastly, contrary to our hypothesis, abundances derived from our analysis of point count data did not closely correlate with the predicted likelihood of Mountain Quail presence from the ARU data. To our

knowledge, this is the first study of Mountain Quail to: investigate habitat relationships of at large landscape scales ≥ 500 m, including relationships with fire; assess the effects of temperature and precipitation anomalies in California; and compare results for point count and ARU monitoring methods.

Spatial scales associated with Mountain Quail

The relationship between habitat and bird density is scale-dependent, with species densities correlating with land cover covariates at both local and landscape scales (Thompson and Mcgarigal 2002, Betts et al. 2014, Stuber and Gruber 2020). Our results illustrate how the effects of scale vary by survey method. Local-scale covariates (50–500 m) typically best represent conditions within a Mountain Quail's large home range, which averaged 141 ha in the southern Cascades of Oregon (Pope et al. 2004), including essential resources such as cover, food, and water-for reproduction. Landscape-scale measures of habitat are more aligned with factors that influence meta-population dynamics and the distribution of resources across broader areas (Saab 1999), including during the non-breeding season. Adequate habitat at these larger scales also increases the likelihood that a patch will be occupied (Hanski 1998, Ovaskainen 2002). Our results suggest that Mountain Quail abundance and presence are driven by environmental covariates across extensive scales, from less than 100 m up to a 5,000 m radius from sample locations.

In our models, local-scale processes best explained variation in abundance, whereas landscape-scale processes better explained variation in presence. This likely reflects both survey protocol differences and the species' ecology. Mountain Quail are highly vocal and can be heard over long distances (Gutiérrez and Delehanty 2020). In the abundance analysis, we truncated detections to within 175 m, which may explain why local-scale covariates (50–500 m) best represented these data. In contrast, the detection distance for ARUs is unknown. Given the species' loud calls, many detections may have occurred beyond 500 m, aligning more closely with landscape-scale covariates. Survey duration also differed between methods. Point counts involved a single 5-minute survey per site per year. Any detection during a point count is more likely to reflect birds within or near the core of their territories, since birds spend most of their time there. ARUs in this study, recorded for six days per site, increasing the likelihood of detecting individuals away from the most frequently used portion of their large territories. It follows that the abundance results would more closely reflect habitat selection within Mountain Quail home ranges (third order of selection), while the presence results better reflect selection of home range placement within a landscape (second order of selection; Johnson 1980).

Processes associated with Mountain Quail

Mountain Quail have been identified as an indicator of early- to mid-seral coniferous forests for the National Forests of the Sierra Nevada Planning Area (USDA Forest Service 2008). Our results support this association, showing correlations with several land cover types and environmental factors characteristic of these forests. Mountain Quails were consistently associated with moderate to high shrub cover across all spatial scales and regions, and at larger scales were

positively associated with low to moderate amounts of tree cover. These findings support previous research on the species throughout their range (Brennan et al. 1987a, Brunk et al. 2023b). Their relationships with land cover and fire variables in the Sierra Nevada specifically suggest Mountain Quail there prefer a relatively active mixed severity fire regime that promotes and retains high shrub cover at local scales, moderate shrub cover at larger scales, and low to moderate tree cover at larger landscape scales. The relationship with pyrodiversity at 6-10 years post fire suggests Mountain Quail are positively associated with burns 6-10 years old that had a relatively uniform burn severity within 100 m of sample locations (Appendix F): abundance peaked at values of pyrodiversity corresponding to 85% of the 100-m radius circle in one severity class and 15% in one other severity class. The relationship with high burn severity at 11-20 years post-fire suggests they continue to use areas within older fires that burned at high severity (Appendix F). However, Mountain Quail tended to be associated with fires 1-5 years old when those fires burned heterogeneously (moderately heterogenous in the Northern Sierra and maximally heterogenous in the Southern Sierra), a burn pattern that would likely retain cover immediately after fire (Appendix F). Our results largely align with those reported by Taillie et al. (2018) and Brunk et al. (Brunk et al. 2023b) in suggesting that Mountain Quail are associated with high severity fires 6-20 years old at local scales less than 500 m, while adding information about the importance of fire severity heterogeneity to promote habitat suitability in the initial years post-fire.

Further study is needed to clarify the role of wildfire on Mountain Quail throughout their range in California, especially given the increasing frequency, severity, and extent of fires across California (Miller and Urban 1999). While fire covariates were not significant outside of the Sierra Nevada region, fire may still be an important driver of Mountain Quail populations in other regions. In the Northern California region, land cover variables – that are in part driven by fire – were better predictors of Mountain Quail distribution than more distal metrics of burn severity and pyrodiversity. Our ARU sample size may have also precluded our ability to detect the effects indexed by the fire covariates by limiting the number of recent fires sampled in the Northern California region.

The climate process models were relatively weak in explaining overall patterns of abundance and presence relative to the land cover and fire process models, yet temperature anomaly covariates had some of the strongest effects on the populations in the final models. Spring snowpack in the Sierra Nevada – commonly measured as April 1 snow water equivalent (SWE) – at elevations below 2500 m is highly sensitive to temperature changes (Howat and Tulaczyk 2005). Warm temperatures enhance snowmelt and cause more precipitation to fall as rain than snow (Kapnick & Hall, 2010, Klos et al., 2014). In a climate simulation study of the Sierra Nevada, Sun et al. (2019) found that at elevations lower than 2,500 m, winter (December through March) mean temperature plays a stronger role than winter accumulated precipitation on April 1 SWE variations. At higher elevations, winter temperatures tend to remain cold enough that precipitation variation is the primary driver of 1 April 1 SWE (Sun et al. 2019). In this context, we interpret the relationships with winter temperature anomalies to mean that Mountain Quail habitat suitability increased with greater snowpack in the Southern Sierra whereas habitat suitability increased with lower snowpack in the Northern Sierra. The large

annual variation in population densities observed in our abundance data in the Southern Sierra suggests that, despite a long-term stable trend, the regional population does fluctuate largely, possibly as a product of climatic variation such as snowpack. It is plausible that the strong elevational gradients in the Southern Sierra selected for by Mountain Quail in that region enable them to find refuge from high snowpack at lower elevations with relatively small movements while also being able to exploit the benefits that high snowpack brings in spring through increased primary productivity and increased availability of water. Mountain Quail in the higher elevation portions of their range are known to move down in elevation during the winter (Gutierrez & Delehanty 2020,). It is also plausible that in the Northern Sierra, where elevation gradients are weaker, finding refuge from high snowpack may require prohibitively long movement, such that when snowpack is high, quail experience increased mortality as has been reported from introduced populations in Idaho and Washington (Stephenson et al. 2011). If this were the case, one would expect the pattern we found of increased abundances in the Northern Sierra following winters with below average snowpack, especially if moisture availability (i.e., spring snowpack) was less of a limiting factor for habitat suitability in this region that is consistently wetter than the Southern Sierra.

Anomalously high summer temperatures also influenced Mountain Quail populations. In the Northern California region, there was a lower likelihood of Mountain Quail presence in the year following anomalously high summer temperatures. Anomalously high temperatures can have direct and indirect negative effects on birds, especially nests and young (Bourne et al. 2020, Conradie et al. 2020, Riggio et al. 2023b). Stephenson et al. (2011) also found that higher spring and summer temperatures reduced Mountain Quail survival. Given projections for increased number and duration of heat waves with climate change, it is possible that Mountain Quail living in areas that are already hotter and closer to their biological thermal limits may experience population declines. In the higher elevations of the Sierra Nevada, however, it is thought that cold spring and summer temperatures are a limiting factor for bird populations (Saracco et al. 2019), which may explain our finding that abundance was higher in the Southern Sierra in areas experiencing anomalously warm summer temperatures, a pattern also observed by Roberts et al. (2019).

Comparison of abundance and presence predictions

Although all abundance and presence models exhibited good fit, there was a very weak relationship between abundance and presence. In the Northern Sierra, for example, abundance and presence were significantly and positively correlated ($p = 0.04$), yet abundance explained less than one percent of the variance in presence. As expected, the correlation was somewhat stronger for survey sites ($R^2 = 0.03$) compared to broader regional predictions ($R^2 = 0.01$) but still not ecologically meaningful. In the Modoc-Cascades, the correlation was weakly negative. While surprising, the poorer correlation relative to the Northern Sierra was expected given that results from the presence model in this analysis were derived from a model for the entire Northern California region whereas the abundance model was specific to the Modoc-Cascades region. Moreover, the abundance and presence results were obtained from point counts and ARUs sampled at different locations from each other.

This pattern is not unique to Mountain Quail. Ten Caten et al. (2022) reported similarly weak associations between abundance and occupancy across multiple taxa, including several breeding landbirds, and Gaston et al. (1999) found no relationship for forest birds.

In our study, weak or absent correlations often coincided with surveys conducted early or late in the season, regardless of whether data came from point counts or ARUs. By contrast, the strongest correlations occurred when both survey types were conducted mid-season. This may reflect seasonal shifts in Mountain Quail behavior or the fact that mid-season surveys were disproportionately conducted at mid-elevations, where snowmelt permitted access. More broadly, the abundance–presence relationship is typically neither constant nor linear, and is known to vary with species, species traits, time (within and across years, length of surveys), habitat, and spatial grain (Gaston et al. 1999, Zuckerberg et al. 2009, Johnston et al. 2015, Steenweg et al. 2018, Manne and Veit 2020, Ten Caten et al. 2022). Our results suggest that a combination of species behavior, sampling design, and/or monitoring protocol may have jointly contributed to the weak relationship observed here.

Densities and trends

Our density estimates decreased from south to north in eastern California, with the highest in the Southern Sierra and the lowest in the Modoc–Cascade region, a pattern also reported by Brennan et al. (1987). However, our breeding season density estimates are at least nine times lower than those recorded three decades ago based on line transect surveys (Brennan et al. 1987b). Although differences in survey methodology may contribute to this discrepancy, significant long-term declines have also been documented in California using Breeding Bird Survey data since 1993 (Sauer et al. 2020). While our results indicate a stable trend from 2010 to 2021, results from the Sierra Nevada and the Modoc-Cascades region incorporating 2024 densities reveal a recent downward shift (Rousseau et al. 2025).

Assumptions and limitations of our approach

Interpreting ARU detections of Mountain Quail requires careful consideration of how call characteristics and habitat affect detection distances. Mountain Quail are vocal with a distinctive song that makes them well-suited for detection. However, the loudness of their song combined with mountainous terrain likely facilitates their detection by ARUs from farther than the distance thresholds typically used in point count surveys and analysis of point count data. At the same time, their preference for dense shrubby habitats and irregular topography, and the unidirectional design of ARUs may reduce detections, particularly when calls originate from behind the unit or a hill. Though these same challenges also affect human observers, people can slightly adjust their position to better estimate the direction and distance of calls. Overall, the uncertainty surrounding the distance at which individual Mountain Quail were being detected by the ARUs translates into uncertainties of the scale at which to interpret presence data.

Another limitation of our approach is the imbalance in sample sizes between ARU and point count survey sites. Although both analyses were based on station-year combinations, the ARU

dataset included only a few hundred records compared to more than 15,000 station-year surveys in the point count dataset. The lower ARU sample size likely constrained the range of covariates represented in the presence models and reduced our ability to accurately predict occurrences across broad spatial extents.

Recommendations for monitoring Mountain Quail

Future monitoring of Mountain Quail should consider sampling designs and protocols that align with the species' ecology, the geography and extent of its distribution, and the data needed to inform management decisions. The findings from long-term ongoing monitoring can track populations and inform management decisions during this time of unprecedented and rapid environmental change (Williams and Brown 2014). Thus, long-term regular monitoring is essential to refining conservation strategies and ensuring management decisions reflect the most current ecological conditions.

Our results suggest that Mountain Quail populations, while largely associated with early- and mid-seral forests, also respond to somewhat different environmental covariates and exhibit variable densities across regions even within their distribution in California. This highlights the importance of avoiding assumptions of stationarity across a species' range and instead taking a regional approach when assessing populations across broad distributions (Fink et al. 2010, Rousseau and Betts 2022). If we had combined all three regions into a single analysis, processes and dynamics associated with high-density areas would likely have overshadowed processes and dynamics in lower-density regions. This indicates that land management or population management strategies for Mountain Quail applied uniformly across California also may not yield consistent outcomes. If possible, future monitoring and management should account for regional variation in habitat associations and population density. Furthermore, geographic areas not included in this study, such as most of the California Coast Ranges and the southern California mountains, should be included in future monitoring efforts. These regions likely support distinct subspecies of Mountain Quail (Gutiérrez and Delehanty 2020), which may differ in their ecology and responses to management.

Because Mountain Quail is a managed game species, obtaining and tracking reliable estimates of abundance across its distribution is essential for informed population management. While technologies such as ARUs offer several benefits, and efforts are underway to derive abundance from them (Fiss et al. 2024), the accuracy of ARU-based abundance estimates varies with species and other factors (Pérez-Granados and Traba 2021, Hutschenreiter et al. 2024, de Araújo et al. 2025). For this reason, point counts remain the recommended sampling protocol for estimating abundance. Point counts are also the recommended protocol when studying a species such as the Mountain Quail that is both frequently heard at most sites and abundant (Doser et al. 2021), since abundance is often more sensitive than presence/absence to environmental changes and often serve as a better indicator of real population declines (Beever et al. 2013, Ashcroft et al. 2017). As such, continuing point count surveys in currently monitored regions and expanding them into new areas would allow managers to assess both long-term population trajectories, compare abundance across regions, and ensure population size targets within regions are being achieved, all necessary information for managers to justify harvest

limits. In addition, long-term monitoring is especially helpful to track populations and inform management decisions during this time of unprecedented and rapid environmental change (Williams and Brown 2014).

Incorporating ARU surveys alongside point counts could provide some important advantages. Integrating data from both methods within a single population model could allow simultaneous evaluation of local- and landscape-scale processes in Mountain Quail habitat selection. Previous studies demonstrate that considering multiple spatial scales improves model fit and ecological inference (Mitchell et al. 2001, Melles et al. 2003, Frey et al. 2012, Grinde and Niemi 2016). ARUs also add temporal depth to the primarily spatial design of point counts, which can improve the accuracy and precision of population estimates (Zipkin et al. 2017, Miller et al. 2019, Grüss and Thorson 2019, Doser et al. 2021). Furthermore, ARU technology and abundance analytical tools are likely to become more reliable over time. Establishing several years of overlap between point counts and ARUs at the same locations would ensure continuity and provide the foundation for incorporating ARU-derived data into long-term abundance analyses (Van Wilgenburg et al. 2017).

Telemetry studies of Mountain Quail across regions in California could also help to inform their management. Telemetry can answer questions about annual and seasonal survival, breeding season home range sizes, movements and habitat selection during the non-breeding season, and habitat associations at finer scales (e.g., nest site selection) than point count and ARU surveys during the breeding season. With respect to our findings, telemetry in the non-breeding season could help to better understand the effects of temperature anomalies on Mountain Quail movement patterns and breeding behaviors.

CONCLUSION

We compared Mountain Quail population estimates from two monitoring methods, point counts and ARUs, and found that the two are not interchangeable but provide complementary insights. Both identified similar land cover types (e.g., shrubs and trees) and environmental drivers (e.g., fire) as important to Mountain Quail but differed in scale and showed relationships that varied across regions. Point counts and abundance were better correlated with local-scale land cover, while ARUs and presence were best explained by landscape-scale land cover. Importantly, population trends derived from both methods were stable and broadly consistent across regions.

These findings suggest that monitoring method selection should depend on study and management goals. Point counts remain the best approach for estimating abundance, particularly where management of a game species is the priority. When land management recommendations are needed, combining both approaches may be the most effective, as they provide complementary information on habitat associations across scales. More broadly, this dual-method framework may strengthen population assessments of species like Mountain Quail, whose distributions span heterogeneous and topographically complex landscapes. While the resulting population trends may seem comparable across methodologies, they reflect

different aspects of the population. Trends in abundance are typically correlated with trends in occurrence, however, the relationship can change or even decouple because of density-dependent processes, mismatches in scales, and changes in habitat quality. As such it is essential to keep the monitoring goal in mind when designing a survey design.

APPENDIX A: Additional species predicted.

Table A-1. Species used to optimize the Mountain Quail predictions, and whether these were positively or negatively correlated with the abundance of Mountain Quails.

Species Name (English, Latin)	Association
Bewick's Wren, *Thryomanes bewicki*	Positive
Black-headed Grosbeak, *Pheucticus melanocephalus*	Positive
California Quail, *Callipepla californica*	Positive
Fox Sparrow, *Passerella iliaca*	Positive
Green-tailed Towhee, *Pipilo chlorurus*	Positive
MacGillivray's Warbler, *Geothlypis tolmiei*	Positive
Nashville Warbler, *Leiothlypis ruficapilla*	Positive
Spotted Towhee, *Pipilo maculatus*	Positive
Steller's Jay, *Cyanocitta stelleri*	Positive
Wrentit, *Chamaea fasciata*	Positive
Brown Creeper, *Certhia americana*	Negative
Gray Flycatcher, *Empidonax wrightii*	Negative
Cassin's Finch, *Haemorhous cassinii*	Negative
Hammond's Flycatcher, *Empidonax hammondii*	Negative
Hermit Thrush, *Catharus guttatus*	Negative
Hermit Warbler, *Setophaga occidentalis*	Negative
Pine Siskin, *Spinus pinus*	Negative
Savannah Sparrow, *Passerculus sandwichensis*	Negative
Western Flycatcher, *Empidonax difficilis*	Negative
Yellow-rumped Warbler, *Setophaga coronata*	Negative

APPENDIX B: Details of the CNN model evaluation step.

To evaluate the performance of the AI model, we compared its predictions against the golden validation dataset. Specifically, we looked for predictions of quail detection from the AI model that occurred within two seconds before or after every annotation in the golden validation dataset. Predictions within this ± 2-second window were classified as true positives. Any predictions outside this window were considered false positives, while instances where experts noted a call but the model did not were counted as false negatives. Among the predictions vs golden validation records comparisons, the false positive predictions had a mean confidence of 0.19, whereas the true positive predictions had mean confidence of 0.57. Though this was an encouraging result, some true positives still received lower confidence scores than certain false positives. To find the penalization threshold that maximized prediction precision (i.e., most predictions being true positives), we varied the penalization level from 0.01 to 0.99 in increments of 0.01. At each penalization level, every prediction below it was ignored. In an ideal classifier, increasing the penalization threshold will increase precision because we filter out less confident predictions and end up with the predictions the model deems most certainly to be quail calls. The downside of a high threshold is that we discard more predictions, and some of these might have been correct, thus increasing the false negative detection rate. Indeed, our analysis confirmed this trade-off. Maximum precision (98%) was obtained with the near maximum threshold of 0.98, but sensitivity (recall) dropped to 20%. While only one false positive remained among the golden validation predictions, we failed to detect 80% of the true detections at that penalization rate. To balance precision and recall, we used the F_β index:

$$F_\beta = (1+\beta)^2 \times \frac{Precision \times Recall}{(\beta^2 \times Precision) + Recall}$$

Increasing values of beta (β) result in higher recall. We used β = 1 to find a penalization threshold. The penalization threshold that maximized F(β=1) (henceforth the maxF1 threshold) was 0.81 and resulted in 75% sensitivity (recall) and 87% precision.

After identifying the maxF1 penalization threshold, we found that the resulting detections still included a 13% false positive rate. To further reduce the rate of false positives while maintaining high recall, we evaluated the detections after the maxF1 penalization against the golden validations, scoring true positives as 1 and false positives as 0. These binary outcomes served as the response variable in a Random Forests model. As model covariates, we used the maximum confidence score at the maxF1 threshold for the 10 species commonly and 10 species unlikely to be found with mountain quail. When a species was not predicted in a recording, its predicted confidence value was set to zero.

Because the number of true positive quail detections is much higher than the number of false positives, fitting an unbalanced model would result in a model that is good at predicting true positives but not adequate at identifying false positives. To address this imbalance, we used a bootstrap procedure where all false positive records were included, and an equal number of

true positives were randomly sampled with replacement. We created 100 bootstrap samples and thus fitted 100 models. Each model was tuned through k-fold cross-validations and tested against a holdout set. We then weighted model predictions by their RMSE and combined them into an ensemble average prediction, representing the probability that a detection was a true positive. Since the ensemble-average prediction is a probability, and since the prediction is for a detection in the golden validation dataset, we found the threshold that maximized the precision of the ensemble-averaged prediction using the same method as described above for finding maxF1 (henceforth the "maxRFPrecision").

In summary, we used the golden validations to find a penalization threshold that maximized the F_β index at $\beta=1$, retaining only predictions above this threshold (the maxF1 threshold). However, because a significant number of false positives remained after maxF1 penalization, we fitted an ensemble of Random Forest models that incorporated information from co-occurring species to help distinguish true from false positives. Ensemble-average predictions, weighted by each model's root mean squared error, were then used to assess whether detections above the maxF1 threshold were true or false positives. We identified the threshold that maximized the validity of the ensemble-averaged predictions (the maxRFPrecision threshold). Any penalized predictions at or above this threshold were deemed true positives, while those below it were discarded.

APPENDIX C: List of covariates considered.

Table B-1. List of covariates considered in the models, their descriptions, spatial and temporal summary, and source.

Covariate †	Description	Spatial grain	Spatial summary	Temporal grain	Temporal summary	Source
Day of year*	Julian day – 1 to 366.	.	.	Daily	Daily	Field data
Time of day*	Time of point count.	.	.	HH:MM	HH:MM	Field data
Observer group*	Point count surveyed by observer in Group A or Group B	.	.	.	.	Point count surveyors were separated into groups. A and B, based on a cluster analysis of their recorded distances to Mountain Quail
Latitude[t]	Latitude at survey location.	30 m	Decimal degree of point	.	.	Field data
Longitude**	Longitude at survey location	30 m	Decimal degree of point		.	
Aspect – North-South [t]	Compass direction facing a slope, where values close to 1 is north facing and -1 is south facing.	30 m	100 m	.	.	The NASA Shuttle Radar Topography Mission (SRTM, see Farr et al. 2007) digital elevation data, extracted through Google Earth Engine
Aspect – East-West [t]	Compass direction facing a slope, where values close to 1 is east facing and -1 is west facing.	30 m	100 m	.	.	The NASA Shuttle Radar Topography Mission (SRTM, see Farr et al. 2007) digital elevation data, extracted through Google Earth Engine
Topographic relief [t]	Standard deviation of the elevation pixels within buffered area.	30 m	100 m, 500 m, and 2000 m	.	.	The NASA Shuttle Radar Topography Mission (SRTM, see Farr et al. 2007) digital elevation data, extracted through Google Earth Engine
Distance to stream [t]	Distance of survey to closest permanent, perennial, or intermittent streams.	Line	Distance to closest in meters	.	.	National Hydrography Dataset
Distance to lakes [t]	Distance of survey to closest permanent, perennial, or intermittent lakes and meadows.	Polygon	Distance to closest in meters	.	.	National Hydrography Dataset
Yearly temperature [t] (index of elevation)	Yearly average of the monthly mean temperature for the months of Jan. to Aug. This covariate is meant to reflect elevation.	4,683 m	500 m	Monthly	Yearly	PRISM Monthly Spatial Climate Dataset AN81m, extracted using Google Earth Engine
Precipitation anomaly and lag by one year of anomaly – winter	Precipitation baseline was calculated using sum of precipitation from Dec. to Feb., averaged across the years of 1981 to 2010. Anomaly is the yearly sum of precipitation minus the baseline.	4,683 m	500 m	Monthly	Yearly	PRISM Monthly Spatial Climate Dataset AN81m, extracted using Google Earth Engine
Temperature anomaly and lag by one year of anomaly – winter	Winter temperature baseline was calculated using minimum monthly temperature from Dec. to Feb., averaged	4,683 m	500 m	Monthly	Yearly	PRISM Monthly Spatial Climate Dataset AN81m, extracted using Google Earth Engine

Covariate †	Description	Spatial grain	Spatial summary	Temporal grain	Temporal summary	Source
	across the years of 1981 to 2010. Anomaly is the yearly average minus the baseline.					
Temperature anomaly and lag by one year of anomaly – summer	Summer temperature baseline was calculated using minimum monthly temperature from June to Aug., averaged across the years of 1981 to 2010. Anomaly is the yearly average minus the baseline.	4,683 m	500 m	Monthly	Yearly	PRISM Monthly Spatial Climate Dataset AN81m, extracted using Google Earth Engine
Percent high burn severity	Percentage of the pixels associated with a high burn category (Composite Burn Index level 4).	30 m	100 m, 250 m, 500 m, 1000 m	Yearly	Previous 1 to 5 years, 6 to 10 years, and 11 to 20 years	Monitoring Trends in Burn Severity (MTBS), extracted using Google Earth Engine
Pyrodiversity	Shannon Index of the diversity of burn severities (categories 0 to 4) and their associated number of pixels.	30 m	100 m, 250 m, 500 m, 1000 m	Yearly	Previous 1 to 5 years, 6 to 10 years, and 11 to 20 years	Monitoring Trends in Burn Severity (MTBS), extracted using Google Earth Engine
Number of years since fire	Number of years since fire, going back to 1990 (maximum 20 years prior to year of survey).	30 m	1000 m	Yearly	Yearly	Monitoring Trends in Burn Severity (MTBS), extracted using Google Earth Engine
Shrub cover	Average and standard deviation of the proportion of shrub canopy within the buffer. Shrub is defined as vegetation with woody stems less than 6-m in height.	30 m	100 m, 250 m, 500 m, 1000 m, 2000 m, 5000 m	Yearly	Yearly	rcmap - MultiResolution Land Characteristics: https://www.mrlc.gov/data/rcmap-shrub-cover
Shrub height**	Average and standard deviation of the height of all shrubs within the buffer.	30 m	100 m, 250 m, 500 m, 1000 m, 2000 m, 5000 m	Yearly	Yearly	rcmap - MultiResolution Land Characteristics: https://www.mrlc.gov/data/rcmap-shrub-height
Tree cover	Average and standard deviation of the proportion of tree canopy within the buffer.	30 m	100 m, 250 m, 500 m, 1000 m, 2000 m, 5000 m	Yearly	Yearly	rcmap - MultiResolution Land Characteristics: https://www.mrlc.gov/data/rcmap-tree-cover
Landsat red band	Average and standard deviation of the near-infrared band value of each pixel, reflecting vegetation's chlorophyll absorption, where low red band values represent high absorption. First took median value from June and July images at each pixel location, then calculated mean and SD across the buffer.	30 m	100 m, 500 m, 1000 m	16 days	Yearly	Landsat 7 and 8 near-infrared band, extracted using Google Earth Engine

Covariate †	Description	Spatial grain	Spatial summary	Temporal grain	Temporal summary	Source
Landsat near-infrared band	Average and standard deviation of the red band value of each pixel, reflecting vegetation's structure and health, where high values represent healthy plants. First took median value from June and July images at each pixel location, then calculated mean and SD across the buffer.	30 m	100 m, 500 m, 1000 m	16 days	Yearly	Landsat 7 and 8 red band, extracted using Google Earth Engine
Shrub cover*	Percentage of an area occupied by vegetation from 0.5 to 3 meters.	50 m	50 m	Yearly	Yearly	Field vegetation surveys
Shrub height*	Estimate to nearest 1 m of the average height of the upper bounds of the shrub layer.	50 m	50 m	Yearly	Yearly	Field vegetation surveys
Tree cover*	Percentage of an area occupied by vegetation taller than 3 meters.	50 m	50 m	Yearly	Yearly	Field vegetation surveys
Tree height*	Estimate to nearest 1 m of the average height of the upper bounds of the tree layer.	50 m	50 m	Yearly	Yearly	Field vegetation surveys
DBH*	Average diameter at breast height of the tree canopy.	50 m	50 m	Yearly	Yearly	Field vegetation surveys
Basal area*	Area occupied by the cross-section of tree trunks and stems at breast height. Is the average of the basal area taken at five points within a 50-m radius circle.	50 m	50 m	Yearly	Yearly	Field vegetation surveys
Number of snags – 10 to 30 cm*	Number of standing dead trees with a trunk diameter between 10 and 30 cm.	50 m	50 m	Yearly	Yearly	Field vegetation surveys
Number of snags – 30 to 60 cm*	Number of standing dead trees with a trunk diameter between 30 and 60 cm.	50 m	50 m	Yearly	Yearly	Field vegetation surveys

† All covariates beside observer group were assessed as a linear and quadratic term in the models.

* Covariates used in the abundance analysis only.

** Covariates used in the presence analysis only.

ŧ Covariates considered in each process model for both the abundance and presence analysis.

APPENDIX D: List of covariates used in each process model, for each region.

Table C-1. List of covariates for the fire process models correlated with Mountain Quail in each region. The models associated with the first two regions are abundance, while the last two are from occurrence models. The linear model (L) and quadratic (Q) model results include the estimate ± SE and the significance level: *** for p-values <= 0.001, ** for p-values <= 0.01, * for p-values <= 0.05, and . for p-values between 0.05 and 0.1.

Process	Covariate	SNS - PC - Fire	SNN - PC - Fire	SNN - ARU - Fire	NCal - ARU - Fire
All	Aspect_EW_100	L: 0.004±0.046 Q: 0.002 ± 0.061	L: -0.110 ± 0.042 ** Q: -0.080 ± 0.041 *		
All	Aspect_SN_100	L: 0.018 ± 0.045 Q: -0.040 ± 0.054			
All	Jul_day	L: -0.249 ± 0.088 ** Q: -0.267 ± 0.048 ***	L: -0.257 ± 0.060 ***	L: -1.014 ± 0.322 ** Q: 0.967 ± 0.383 *	L: -2.965 ± 0.550 *** Q: -2.027 ± 0.430 ***
All	Latitude	L: -0.315 ± 0.135 * Q: -0.328 ± 0.111 **	L: -0.429 ± 0.065 ***		
All	distLakes	L: -0.069 ± 0.082	L: 0.171 ± 0.088 . Q: -0.055 ± 0.045		
All	temp_avg	L: 0.284 ± 0.111 *	L: -0.430 ± 0.084 ***		
Fire	HighBurn_11to20yrs_250m	L: 0.047 ± 0.016 **	L: 0.270 ± 0.149 . Q: -0.021 ± 0.015		
Fire	HighBurn_6to10yrs_1000m		L: -0.137 ± 0.138 Q: 0.007 ± 0.011		
Fire	Pyro_11to20yrs_100m		L: 0.016 ± 0.117 Q: 0.006 ± 0.017		
FIre	Pyro_11to20yrs_1000m			L: 3.194 ± 5.333	
Fire	Pyro_1to5yrs_1000m	L: -0.322 ± 0.141 * Q: 0.133 ± 0.041 **	L: 0.614 ± 0.221 ** Q: -0.132 ± 0.053 *		
Fire	Pyro_1to5yrs_500m				L: 0.638 ± 0.406
Fire	Pyro_6to10yrs_100m	L: 0.344 ± 0.119 ** Q: -0.059 ± 0.020 **	L: 0.590 ± 0.159 *** Q: -0.088 ± 0.025 ***		
Fire	YrsSinceFire		L: -1.364 ± 0.590 * Q: -0.867 ± 0.368 *		

Table C-2. List of covariates for the local land cover process models correlated with Mountain Quail in each region. The models associated with the first two regions are abundance, while the last two are from occurrence models. The linear model (L) and quadratic (Q) model results include the estimate ± SE and the significance level: *** for p-values <= 0.001, ** for p-values <= 0.01, * for p-values <= 0.05, and . for p-values between 0.05 and 0.1.

Process	Covariate	SNS - PC - Local	SNN - PC - Local	SNN - ARU - Local	NCal - ARU - Local
All	Aspect_EW_100	L: 0.048 ± 0.050 Q: -0.069 ± 0.066	L: -0.210 ± 0.044 *** Q: -0.106 ± 0.042 *		
All	Aspect_SN_100	L: 0.055 ± 0.048 Q: -0.110 ± 0.060 .			
All	ElevSD_100			L: 1.634 ± 0.908 .	
All	ElevSD_500	L: 0.268 ± 0.078 *** Q: -0.129 ± 0.040 **	L: 0.095 ± 0.055 . Q: -0.044 ± 0.028		
All	Jul_day	L: 0.297 ± 0.330 Q: -0.200 ± 0.080 *	L: -0.278 ± 0.059 ***	L: -3.416 ± 1.394 * Q: 1.634 ± 0.771 *	L: -3.776 ± 0.786 *** Q: -2.258 ± 0.535 ***
All	Latitude	L: -0.083 ± 0.132 Q: -0.175 ± 0.111	L: -0.279 ± 0.064 ***		
All	distLakes	L: -0.022 ± 0.080	L: 0.113 ± 0.082 Q: -0.018 ± 0.037		
All	temp_avg	L: 0.229 ± 0.111 *	L: -0.408 ± 0.082 ***		
Local	ShrubCover_mean_100				L: 2.426 ± 1.453
Local	ShrubCover_mean_250	L: 0.040 ± 0.064 Q: 0.053 ± 0.044	L: 0.225 ± 0.081 ** Q: -0.077 ± 0.031 *		
Local	ShrubCover_mean_500			L: 4.797 ± 2.339 * Q: -2.599 ± 0.903 **	
Local	ShrubCover_sd_100	L: -0.012 ± 0.046	L: 0.058 ± 0.082 Q: -0.032 ± 0.032		
Local	ShrubCover_sd_500			L: -4.544 ± 1.877 *	
Local	ShrubHeight_mean_100				L: -3.494 ± 1.562 .
Local	ShrubHeight_mean_250			L: -11.508 ± 4.991 * Q: 0.775 ± 0.379 *	
Local	ShrubHeight_mean_500			L: 10.855 ± 3.907 **	
Local	ShrubHeight_sd_250			L: -3.306 ± 2.607 Q: 3.045 ± 1.266 *	
Local	Shrub_CDL_50		L: 0.030 ± 0.047	L: -0.837 ± 1.755 Q: 2.851 ± 1.517 .	
Local	mean_nir_100		L: 0.205 ± 0.055 *** Q: -0.014 ± 0.023		

Process	Covariate	SNS - PC - Local	SNN - PC - Local	SNN - ARU - Local	NCal - ARU - Local
Local	mean_nir_500			L: -7.920 ± 3.535 *	L: -2.115 ± 0.783 *
Local	mean_red_100	L: -0.083 ± 0.062 Q: -0.054 ± 0.035	L: 0.192 ± 0.068 ** Q: -0.100 ± 0.029 ***	L: -0.924 ± 1.754 Q: -3.231 ± 1.017 **	
Local	mean_red_500				L: -1.572 ± 0.931 Q: 0.655 ± 0.397
Local	sd_nir_100			L: 3.374 ± 1.571 * Q: -2.859 ± 0.982 **	
Local	sd_nir_500	L: 0.232 ± 0.070 ** Q: -0.050 ± 0.022 *	L: 0.124 ± 0.068 . Q: -0.047 ± 0.030	L: 2.327 ± 1.390 .	L: 1.219 ± 0.783
Local	sd_red_100			L: 1.872 ± 1.170	
Local	sd_red_500		L: 0.199 ± 0.088 * Q: -0.063 ± 0.035 .		
Local	shrubcov	L: 0.091 ± 0.041 *	L: 0.214 ± 0.054 *** Q: -0.055 ± 0.028 *		
Local	shrubhtavg	L: 0.079 ± 0.055 Q: -0.029 ± 0.020	L: -0.004 ± 0.040		
Local	snags3060		L: -0.006 ± 0.089 Q: -0.022 ± 0.022		
Local	totdbhmax		L: -0.026 ± 0.038 Q: 0.015 ± 0.018		
Local	treeCover_mean_250			L: -6.791 ± 2.743 * Q: -2.615 ± 1.254 *	
Local	treeCover_sd_500	L: -0.145 ± 0.060 *	L: -0.145 ± 0.067 * Q: -0.111 ± 0.040 **		L: 0.856 ± 0.521
Local	treehtavg	L: -0.039 ± 0.041 Q: 0.020 ± 0.026			

Table C-3. List of covariates for the landscape land cover process models correlated with Mountain Quail in each region. The models associated with the first two regions are abundance, while the last two are from occurrence models. The linear model (L) and quadratic (Q) model results include the estimate ± SE and the significance level: *** for p-values <= 0.001, ** for p-values <= 0.01, * for p-values <= 0.05, and . for p-values between 0.05 and 0.1.

Process	Covariate	SNS - PC – Landscape	SNN - PC - Landscape	SNN - ARU - Landscape	NCal - ARU - Landscape
All	Aspect_EW_100	L: -0.005 ± 0.049 Q: -0.017 ± 0.061	L: -0.117 ± 0.042 ** Q: -0.101 ± 0.041 *		
All	Aspect_SN_100	L: 0.029 ± 0.045 Q: -0.057 ± 0.054			
All	ElevSD_100			L: 2.129 ± 0.871 * Q: -1.802 ± 1.043 .	
All	Jul_day	L: -0.240 ± 0.091 ** Q: -0.286 ± 0.048 ***	L: -0.249 ± 0.059 ***	L: -2.021 ± 0.712 **	L: -3.294 ± 0.657 *** Q: -2.135 ± 0.501 ***
All	Latitude	L: -0.167 ± 0.139 Q: -0.242 ± 0.124 .	L: -0.318 ± 0.078 ***		
All	distLakes	L: -0.010 ± 0.080	L: 0.151 ± 0.087 . Q: -0.062 ± 0.044		
All	temp_avg	L: 0.132 ± 0.116	L: -0.421 ± 0.096 ***		
Landscape	ElevSD_2000	L: 0.302 ± 0.083 *** Q: -0.111 ± 0.046 *			
Landscape	ShrubCover_mean_2000			L: -5.652 ± 3.339 .	L: 2.132 ± 1.254
Landscape	ShrubCover_mean_5000	L: 0.042 ± 0.073 Q: -0.037 ± 0.047	L: 0.170 ± 0.078 * Q: -0.077 ± 0.044 .	L: 1.235 ± 4.018 Q: -2.643 ± 1.465 .	
Landscape	ShrubCover_sd_1000	L: 0.051 ± 0.063	L: 0.085 ± 0.074 Q: -0.082 ± 0.039 *	L: -7.259 ± 2.981 *	
Landscape	ShrubCover_sd_2000			L: 7.318 ± 3.725 * Q: 6.972 ± 2.440 **	
Landscape	ShrubHeight_mean_1000			L: 4.444 ± 2.470 .	
Landscape	ShrubHeight_mean_2000				L: -2.502 ± 1.067 *
Landscape	ShrubHeight_sd_2000			L: -0.739 ± 1.871 Q: -4.290 ± 1.380 **	
Landscape	mean_nir_1000	L: 0.072 ± 0.087	L: 0.269 ± 0.058 ***		L: -1.656 ± 0.816 .
Landscape	mean_red_1000	L: 0.038 ± 0.082 Q: -0.039 ± 0.039	L: 0.302 ± 0.100 ** Q: -0.100 ± 0.036 **		
Landscape	sd_nir_1000	L: 0.153 ± 0.078 * Q: -0.053 ± 0.024 *		L: 2.606 ± 0.987 ** Q: -1.711 ± 0.989 .	L: 1.682 ± 0.725 *
Landscape	sd_red_1000		L: -0.082 ± 0.095		

Landscape	treeCover_mean_1000			L: 2.487 ± 2.399 Q: -6.315 ± 2.053 **	
Landscape	treeCover_mean_2000			L: -13.781 ± 4.945 **	L: 0.318 ± 0.781 Q: 0.590 ± 0.425
Landscape	treeCover_mean_5000		L: -0.089 ± 0.073	L: 4.678 ± 2.287 *	
Landscape	treeCover_sd_1000			L: -3.464 ± 1.423 *	
Landscape	treeCover_sd_5000	L: -0.171 ± 0.073 *	L: -0.137 ± 0.068 *		L: 0.849 ± 0.494

Table C-4. List of covariates for the climate process models correlated with Mountain Quail in each region. The models associated with the first two regions are abundance, while the last two are from occurrence models. The linear model (L) and quadratic (Q) model results include the estimate ± SE and the significance level: *** for p-values <= 0.001, ** for p-values <= 0.01, * for p-values <= 0.05, and . for p-values between 0.05 and 0.1.

Process	Covariate	SNS - PC - Climate	SNN - PC - Climate	SNN - ARU - Climate	NCal - ARU - Climate
All	Aspect_EW_100	L: -0.001 ± 0.046 Q: 0.007 ± 0.061	L: -0.103 ± 0.042 * Q: -0.083 ± 0.041 *		
All	Aspect_SN_100	L: 0.040 ± 0.045 Q: -0.041 ± 0.054			
All	ElevSD_100			L: 0.422 ± 0.376 Q: -0.820 ± 0.483 .	
All	Jul_day	L: -0.276 ± 0.076 *** Q: -0.270 ± 0.048 ***	L: -0.276 ± 0.060 ***	L: -1.347 ± 0.356 ***	L: -3.610 ± 0.734 *** Q: -2.449 ± 0.557 ***
All	Latitude	L: -0.107 ± 0.124 Q: 0.010 ± 0.114	L: -0.452 ± 0.069 ***		
All	distLakes	L: -0.083 ± 0.081	L: 0.224 ± 0.093 * Q: -0.063 ± 0.047		
All	temp_avg	L: 0.293 ± 0.098 **	L: -0.466 ± 0.089 ***		
Climate	ppt_anomaly				L: 0.623 ± 0.758 Q: -1.219 ± 0.635 .
Climate	ppt_anomaly_lag1yr	L: -0.268 ± 0.139 .	L: -0.112 ± 0.092 Q: 0.010 ± 0.041		L: -1.395 ± 0.963 Q: 1.497 ± 0.705 .
Climate	tmn_anomaly	L: -0.358 ± 0.130 **	L: 0.138 ± 0.116		
Climate	tmn_anomaly^2		Q: 0.204 ± 0.058 ***		
Climate	tmn_anomaly_lag1yr	L: -0.370 ± 0.132 **	L: -0.029 ± 0.120		L: 0.164 ± 1.300 Q: 2.259 ± 1.098 .
Climate	tmx_anomaly	L: 0.158 ± 0.085 .	L: 0.031 ± 0.125	L: -20.802 ± 8.065 ** Q: 5.816 ± 2.308 *	L: 0.905 ± 0.593
Climate	tmx_anomaly_lag1yr			L: -3.393 ± 1.393 *	L: -0.842 ± 0.688

APPENDIX E. Spatial autocorrelation plots.

Figure D-1. Moran's I spatial autocorrelation index across distances for the Modoc-Cascades region.

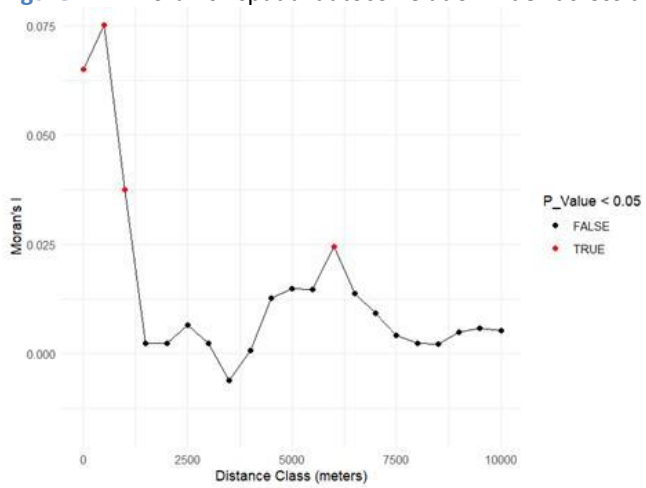

Figure D-2. Moran's I spatial autocorrelation index across distances for the Northern Sierra region.

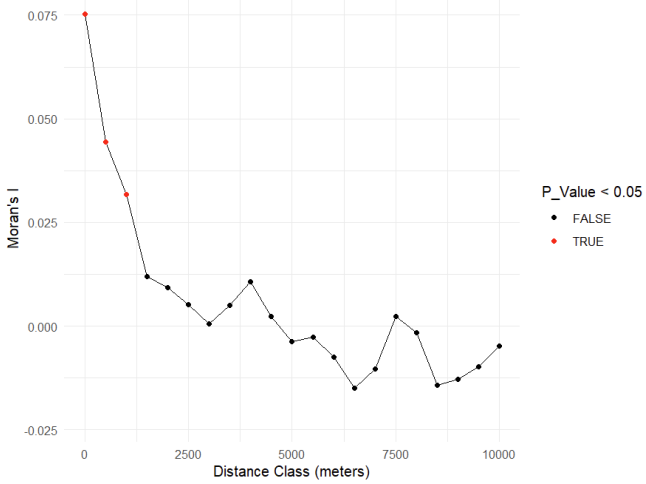

Figure D-3. Moran's I spatial autocorrelation index across distances for the Southern Sierra region.

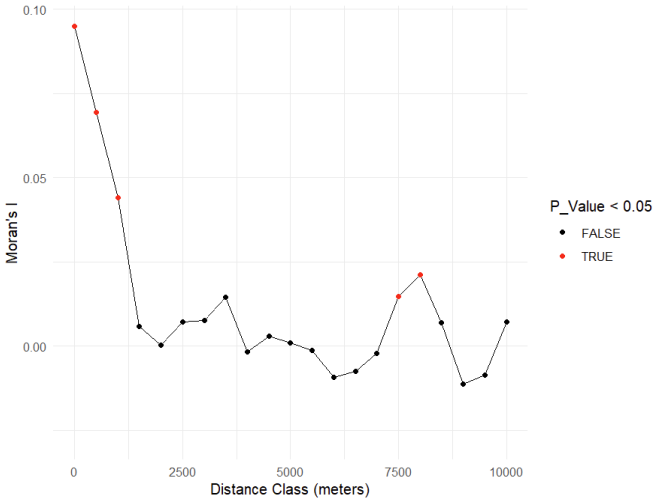

APPENDIX F. Partial dependence plots.

Figure F-1. Partial dependence plots associated with the Mountain Quail, for the fire and climate processes, per region and model.

Southern Sierra – Abundance model – Fire covariates

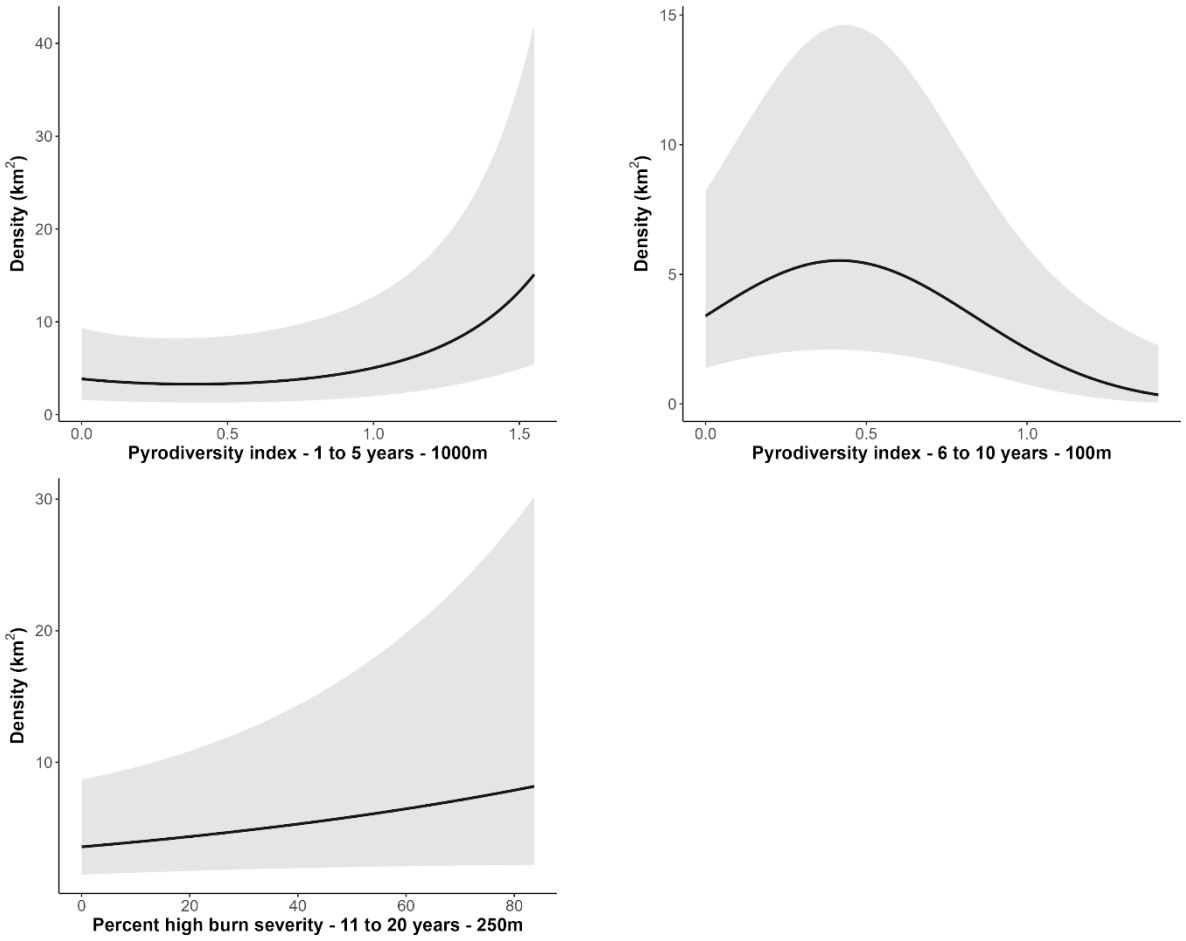

Southern Sierra – Abundance model – Climate covariates

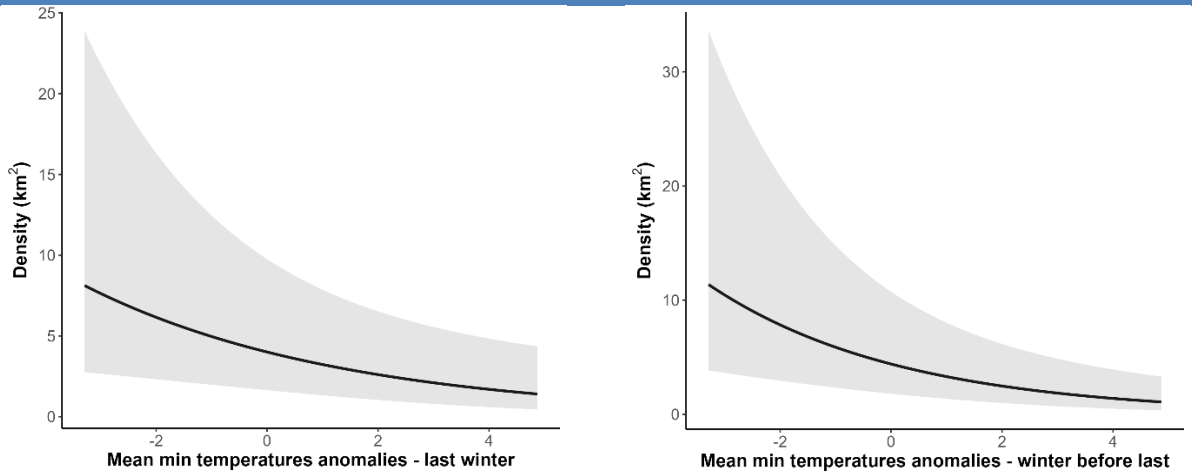

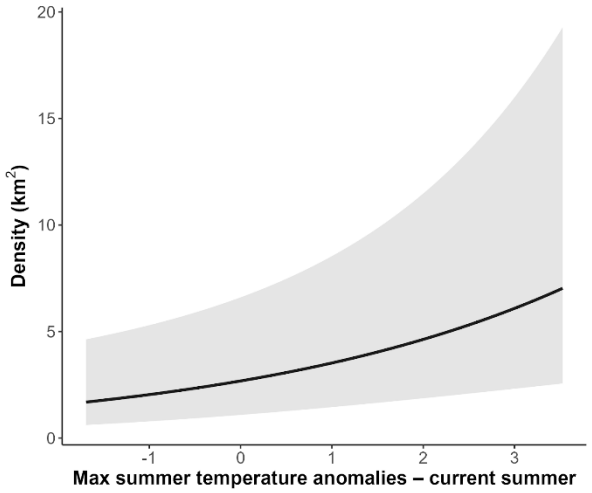

Northern Sierra – Abundance model – Fire covariates

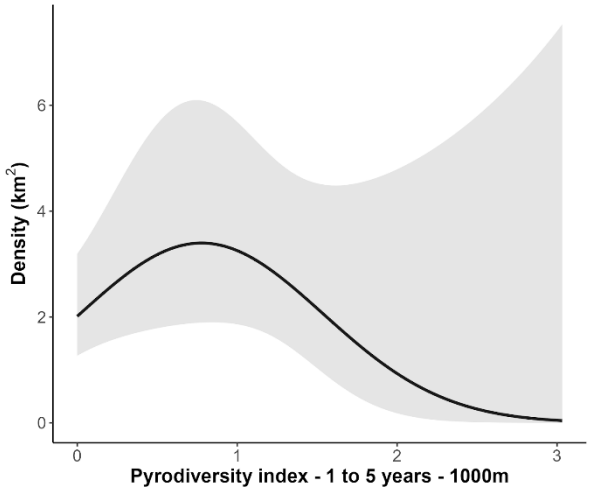

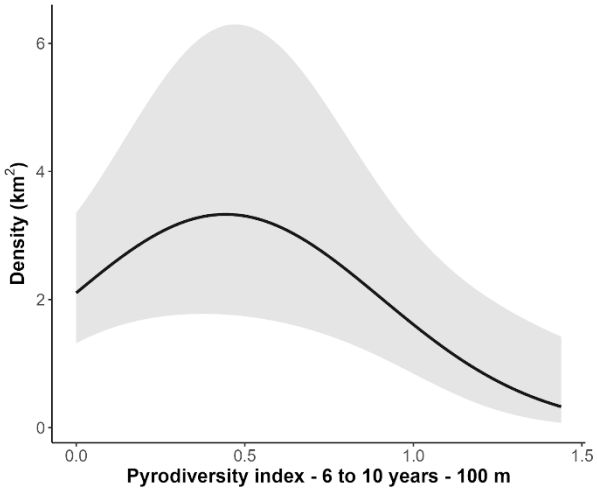

Northern Sierra – Abundance model – Climate covariates

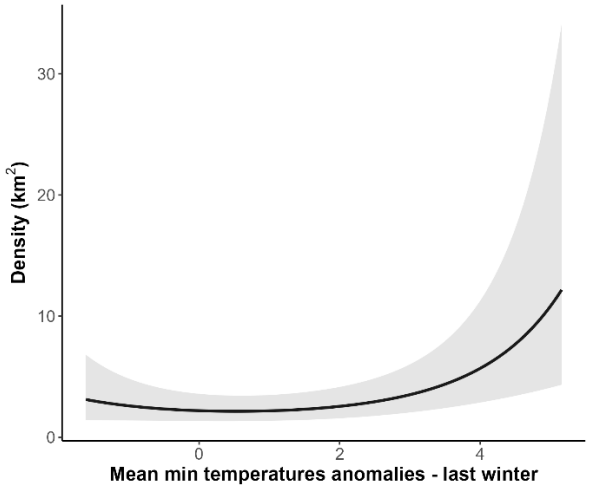

Northern Sierra – Presence model – Fire covariates

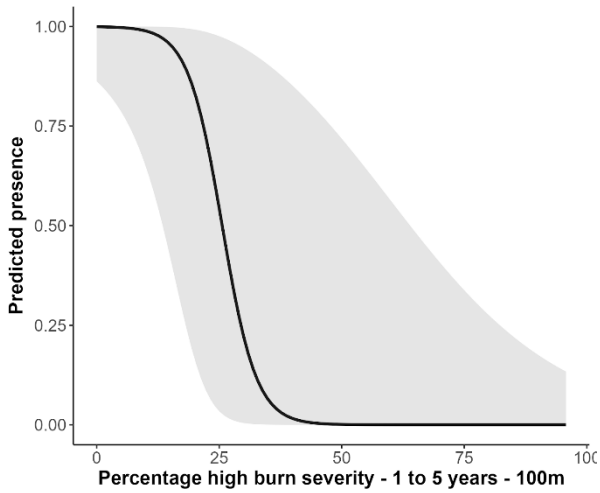

Northern California – Presence model – Climate covariates

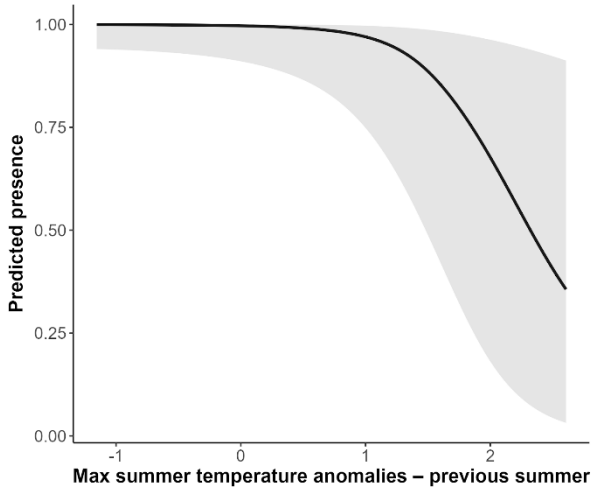

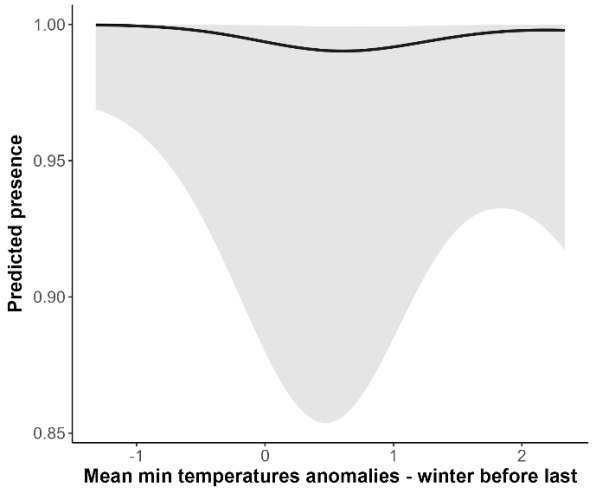

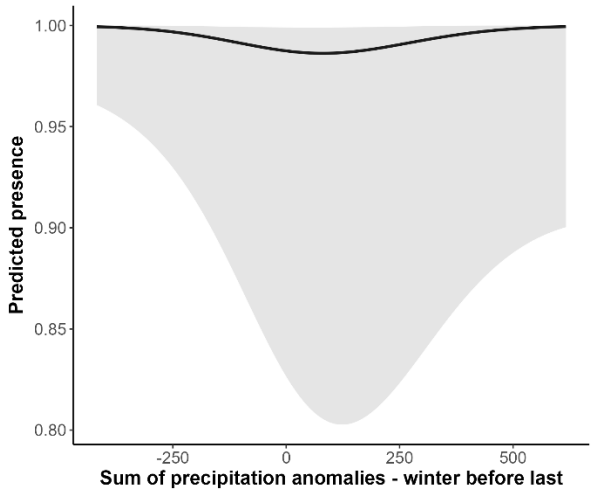

REFERENCES

Aide, T. M., C. Corrada-Bravo, M. Campos-Cerqueira, C. Milan, G. Vega, and R. Alvarez. 2013. Real-time bioacoustics monitoring and automated species identification. PeerJ 1:e103.

Akinwande, M. O., H. G. Dikko, and A. Samson. 2015. Variance Inflation Factor: As a Condition for the Inclusion of Suppressor Variable(s) in Regression Analysis. Open Journal of Statistics 05:754.

de Araújo, C. B., H. S. Oliveira, J. P. Zurano, G. L. M. Rosa, C. R. M. A. Simões, G. A. Zurita, and L. dos Anjos. 2025. Towards large-scale abundance assessments through automated birdsong detection and distance estimation. Ibis.

Ashcroft, M. B., D. H. King, B. Raymond, J. D. Turnbull, J. Wasley, and S. A. Robinson. 2017. Moving beyond presence and absence when examining changes in species distributions. Global Change Biology 23:2929–2940.

Bahn, V., R. J. O'Connor, and W. B. Krohn. 2006. Importance of spatial autocorrelation in modeling bird distributions at a continental scale. Ecography 29:835–844.

Baldwin, R. W., J. T. Beaver, M. Messinger, J. Muday, M. Windsor, G. D. Larsen, M. R. Silman, and T. M. Anderson. 2023. Camera Trap Methods and Drone Thermal Surveillance Provide Reliable, Comparable Density Estimates of Large, Free-Ranging Ungulates. Animals 13:1884.

Beever, E. A., S. Z. Dobrowski, J. Long, A. R. Mynsberge, and N. B. Piekielek. 2013. Understanding relationships among abundance, extirpation, and climate at ecoregional scales. Ecology 94:1563–1571.

Bentz, B. J., J. Régnière, C. J. Fettig, E. M. Hansen, J. L. Hayes, J. A. Hicke, R. G. Kelsey, J. F. Negrón, and S. J. Seybold. 2010. Climate Change and Bark Beetles of the Western United States and Canada: Direct and Indirect Effects.

Betts, M. G., A. W. Diamond, G. J. Forbes, M.-A. Villard, and J. S. Gunn. 2006. The importance of spatial autocorrelation, extent and resolution in predicting forest bird occurrence. Ecological Modelling 191:197–224.

Betts, M. G., L. Fahrig, A. S. Hadley, K. E. Halstead, J. Bowman, W. D. Robinson, J. A. Wiens, and D. B. Lindenmayer. 2014. A species-centered approach for uncovering generalities in organism responses to habitat loss and fragmentation. Ecography 37:517–527.

Block, W. M., L. A. Brennan, and R. J. Gutiérrez. 1987. Evaluation of guild-indicator species for use in resource management. Environmental Management 11:265–269.

Bourne, A. R., S. J. Cunningham, C. N. Spottiswoode, and A. R. Ridley. 2020. High temperatures drive offspring mortality in a cooperatively breeding bird. Proceedings of the Royal Society B: Biological Sciences 287:20201140.

Brennan, L. A., W. M. Block, and R. J. Gutierrez. 1987a. Habitat Use by Mountain Quail in Northern California. The Condor 89:66.

Brennan, L. A., W. M. Block, and R. J. Gutierrez. 1987b. Habitat Use by Mountain Quail in Northern California. The Condor 89:66.

Brunk, K. M., J. F. Goldberg, C. Maxwell, M. Z. Peery, G. M. Jones, L. R. Gallagher, H. A. Kramer, A. L. Westerling, J. J. Keane, S. Kahl, and C. M. Wood. 2025. Bioregional-scale acoustic monitoring can support fire-prone forest restoration planning. Frontiers in Ecology and the Environment:e2843.

Brunk, K. M., R. J. Gutiérrez, M. Z. Peery, C. A. Cansler, S. Kahl, and C. M. Wood. 2023a. Quail on fire: changing fire regimes may benefit mountain quail in fire-adapted forests. Fire Ecology 19:19.

Brunk, K. M., R. J. Gutiérrez, M. Z. Peery, C. A. Cansler, S. Kahl, and C. M. Wood. 2023b. Quail on fire: changing fire regimes may benefit mountain quail in fire-adapted forests. Fire Ecology 19:19.

Burnham, K. P., and D. R. Anderson. 2004. Multimodel Inference: Understanding AIC and BIC in Model Selection. Sociological Methods & Research 33:261–304.

Clark, M. L., L. Salas, S. Baligar, C. A. Quinn, R. L. Snyder, D. Leland, W. Schackwitz, S. J. Goetz, and S. Newsam. 2023. The effect of soundscape composition on bird vocalization classification in a citizen science biodiversity monitoring project. Ecological Informatics 75:102065.

Conradie, S. R., S. M. Woodborne, B. O. Wolf, A. Pessato, M. M. Mariette, and A. E. McKechnie. 2020. Avian mortality risk during heat waves will increase greatly in arid Australia during the 21st century. Conservation Physiology 8:coaa048.

Cunningham, M. A., and D. H. Johnson. 2006. Proximate and landscape factors influence grassland bird distributions. Ecological Applications: A Publication of the Ecological Society of America 16:1062–1075.

Dalton, D. T., K. Pascher, V. Berger, K. Steinbauer, and M. Jungmeier. 2022. Novel Technologies and Their Application for Protected Area Management: A Supporting Approach in Biodiversity Monitoring. Page *in* M. Nazip Suratman, editor. Protected Area Management - Recent Advances. IntechOpen.

Darras, K., P. Batáry, B. Furnas, A. Celis-Murillo, S. L. Van Wilgenburg, Y. A. Mulyani, and T. Tscharntke. 2018. Comparing the sampling performance of sound recorders versus point counts in bird surveys: A meta-analysis. Journal of Applied Ecology 55:2575–2586.

DeLeon, E. E., M. W. Hook, M. F. Small, and A. K. Tegeler. 2023. Comparing and combining use of autonomous recording units and traditional counts to monitor Northern Bobwhite. Journal of Field Ornithology 94.

Doser, J. W., A. O. Finley, A. S. Weed, and E. F. Zipkin. 2021. Integrating automated acoustic vocalization data and point count surveys for estimation of bird abundance. Methods in Ecology and Evolution 12:1040–1049.

Drake, A., D. R. de Zwaan, T. A. Altamirano, S. Wilson, K. Hick, C. Bravo, J. T. Ibarra, and K. Martin. 2021. Combining point counts and autonomous recording units improves avian survey efficacy across elevational gradients on two continents. Ecology and Evolution 11:8654–8682.

Dugger, K. M., E. D. Forsman, A. B. Franklin, R. J. Davis, G. C. White, C. J. Schwarz, K. P. Burnham, J. D. Nichols, J. E. Hines, C. B. Yackulic, P. F. Doherty, L. Bailey, D. A. Clark, S. H. Ackers, L. S. Andrews, B. Augustine, B. L. Biswell, J. Blakesley, P. C. Carlson, M. J. Clement, L. V. Diller, E. M. Glenn, A. Green, S. A. Gremel, D. R. Herter, J. M. Higley, J. Hobson, R. B. Horn, K. P. Huyvaert, C. McCafferty, T. McDonald, K. McDonnell, G. S. Olson, J. A. Reid, J. Rockweit, V. Ruiz, J. Saenz, and S. G. Sovern. 2016. The effects of habitat, climate, and Barred Owls on long-term demography of Northern Spotted Owls.

Fettig, C. J., L. A. Mortenson, B. M. Bulaon, and P. B. Foulk. 2019. Tree mortality following drought in the central and southern Sierra Nevada, California, U.S. Forest Ecology and Management 432:164–178.

Fink, D., W. M. Hochachka, B. Zuckerberg, D. W. Winkler, B. Shaby, M. A. Munson, G. Hooker, M. Riedewald, D. Sheldon, and S. Kelling. 2010. Spatiotemporal exploratory models for broad-scale survey data. Ecological Applications 20:2131–2147.

Fiske, I., and R. Chandler. 2011. unmarked : An *R* Package for Fitting Hierarchical Models of Wildlife Occurrence and Abundance. Journal of Statistical Software 43.

Fiss, C. J., S. Lapp, J. B. Cohen, H. A. Parker, J. T. Larkin, J. L. Larkin, and J. Kitzes. 2024. Performance of unmarked abundance models with data from machine-learning classification of passive acoustic recordings. Ecosphere 15:e4954.

Fortin, M.-J., P. Drapeau, and P. Legendre, editors. 1989. Spatial autocorrelation and sampling design in plant ecology. Progress in theoretical vegetation science 83:209–222.

Frey, S. J. K., A. M. Strong, and K. P. McFarland. 2012. The relative contribution of local habitat and landscape context to metapopulation processes: a dynamic occupancy modeling approach. Ecography 35:581–589.

Fuller, A. K., D. W. Linden, and J. A. Royle. 2016. Management decision making for fisher populations informed by occupancy modeling. The Journal of Wildlife Management 80:794–802.

Furnas, B. J. 2020. Rapid and varied responses of songbirds to climate change in California coniferous forests. Biological Conservation 241:108347.

Furnas, B. J., and R. L. Callas. 2015. Using automated recorders and occupancy models to monitor common forest birds across a large geographic region. The Journal of Wildlife Management 79:325–337.

Gaines, W. L., P. F. Hessburg, G. H. Aplet, P. Henson, S. J. Prichard, D. J. Churchill, G. M. Jones, D. J. Isaak, and C. Vynne. 2022. Climate change and forest management on federal lands in the Pacific Northwest, USA: Managing for dynamic landscapes. Forest Ecology and Management 504:119794.

Gaston, K. J., T. M. Blackburn, and R. D. Gregory. 1999. Intraspecific abundance–occupancy relationships: case studies of six bird species in Britain. Diversity and Distributions 5:197–212.

Goudey, C. B., D. W. Smith, D. T. Cleland, J. A. Freeouf, J. E. Keys Jr., G. J. Nowacki, C. Carpenter, and W. H. McNab. 2007. Ecological Subregions: Sections and Subsections of the Conterminous United States.

Graf, R. F., K. Bollmann, W. Suter, and H. Bugmann. 2005. The Importance of Spatial Scale in Habitat Models: Capercaillie in the Swiss Alps. Landscape Ecology 20:703–717.

Grinde, A. R., and G. J. Niemi. 2016. Influence of landscape, habitat, and species co-occurrence on occupancy dynamics of Canada Warblers. The Condor:513–531.

Grüss, A., and J. T. Thorson. 2019. Developing spatio-temporal models using multiple data types for evaluating population trends and habitat usage. ICES Journal of Marine Science 76:1748–1761.

Gutiérrez, R. J., and D. J. Delehanty. 2020. Mountain Quail (Oreortyx pictus), version 1.0. Cornell Lab of Ornithology, Ithaca, NY, USA.

Hagmann, R. K., P. F. Hessburg, S. J. Prichard, N. A. Povak, P. M. Brown, P. Z. Fulé, R. E. Keane, E. E. Knapp, J. M. Lydersen, K. L. Metlen, M. J. Reilly, A. J. Sánchez Meador, S. L. Stephens, J. T. Stevens, A. H. Taylor, L. L. Yocom, M. A. Battaglia, D. J. Churchill, L. D. Daniels, D. A. Falk, P. Henson, J. D. Johnston, M. A. Krawchuk, C. R. Levine, G. W. Meigs, A. G. Merschel, M. P. North, H. D. Safford, T. W. Swetnam, and A. E. M. Waltz. 2021. Evidence for widespread changes in the structure, composition, and fire regimes of western North American forests. Ecological Applications 31:e02431.

Halofsky, J. E., D. L. Peterson, and B. J. Harvey. 2020. Changing wildfire, changing forests: the effects of climate change on fire regimes and vegetation in the Pacific Northwest, USA. Fire Ecology 16:4.

Halofsky, J., and D. Peterson. 2016. Climate change vulnerabilities and adaptation options for forest vegetation management in the northwestern USA. Atmosphere. 7(3): 46-. 7:46.

Halsch, C. A., A. M. Shapiro, J. H. Thorne, K. C. Rodman, A. Parra, L. A. Dyer, Z. Gompert, A. M. Smilanich, and M. L. Forister. 2024. Thirty-six years of butterfly monitoring, snow cover, and plant productivity reveal negative impacts of warmer winters and increased productivity on montane species. Global Change Biology 30:e17044.

Hanski, I. 1998. Metapopulation dynamics. Nature 396:41.

Hessburg, P. F., T. A. Spies, D. A. Perry, C. N. Skinner, A. H. Taylor, P. M. Brown, S. L. Stephens, A. J. Larson, D. J. Churchill, N. A. Povak, P. H. Singleton, B. McComb, W. J. Zielinski, B. M. Collins, R. B. Salter, J. J. Keane, J. F. Franklin, and G. Riegel. 2016. Tamm Review: Management of mixed-severity fire regime forests in Oregon, Washington, and Northern California. Forest Ecology and Management 366:221–250.

Hill, A. P., P. Prince, E. Piña Covarrubias, C. P. Doncaster, J. L. Snaddon, and A. Rogers. 2018. AudioMoth: Evaluation of a smart open acoustic device for monitoring biodiversity and the environment. Methods in Ecology and Evolution 9:1199–1211.

Hill, A. P., P. Prince, J. L. Snaddon, C. P. Doncaster, and A. Rogers. 2019. AudioMoth: A low-cost acoustic device for monitoring biodiversity and the environment. HardwareX 6:e00073.

Hodgson, J. C., R. Mott, S. M. Baylis, T. T. Pham, S. Wotherspoon, A. D. Kilpatrick, R. Raja Segaran, I. Reid, A. Terauds, and L. P. Koh. 2018. Drones count wildlife more accurately and precisely than humans. Methods in Ecology and Evolution 9:1160–1167.

Hosmer, D. W., T. Hosmer, S. Le Cessie, and S. Lemeshow. 1997. A comparison of goodness-of-fit tests for the logistic regression model. Statistics in Medicine 16:965–980.

Hosmer, D. W., and S. Lemesbow. 1980. Goodness of fit tests for the multiple logistic regression model. Communications in Statistics - Theory and Methods 9:1043–1069.

Hutschenreiter, A., E. Andresen, M. Briseño-Jaramillo, A. Torres-Araneda, E. Pinel-Ramos, J. Baier, and F. Aureli. 2024. How to count bird calls? Vocal activity indices may provide different insights into bird abundance and behaviour depending on species traits. Methods in Ecology and Evolution 15:1071–1083.

Hutto, R. L., and R. Stutzman. 2009. Humans versus autonomous recording units: a comparison of point-count results. Journal of Field Ornithology 80:387–398.

Johnston, A., D. Fink, M. D. Reynolds, W. M. Hochachka, B. L. Sullivan, N. E. Bruns, E. Hallstein, M. S. Merrifield, S. Matsumoto, and S. Kelling. 2015. Abundance models improve spatial and temporal prioritization of conservation resources. Ecological Applications 25:1749–1756.

Kahl, S., C. M. Wood, M. Eibl, and H. Klinck. 2021. BirdNET: A deep learning solution for avian diversity monitoring. Ecological Informatics 61:101236.

Lewis, W. B., C. Johnson, and J. A. Martin. 2025. Assessing the efficacy and cost-effectiveness of integrating autonomous recording units and point-count surveys for population monitoring of northern bobwhite (Colinus virginianus). Ecological Solutions and Evidence 6:e70056.

Madakumbura, G. D., M. L. Goulden, A. Hall, R. Fu, M. A. Moritz, C. D. Koven, L. M. Kueppers, C. A. Norlen, and J. T. Randerson. 2020. Recent California tree mortality portends future increase in drought-driven forest die-off. Environmental Research Letters 15:124040.

Mallek, C., H. Safford, J. Viers, and J. Miller. 2013. Modern departures in fire severity and area vary by forest type, Sierra Nevada and southern Cascades, California, USA. Ecosphere 4:1–28.

Manne, L. L., and R. R. Veit. 2020. Temporal changes in abundance–occupancy relationships over 40 years. Ecology and Evolution 10:602–611.

McGinn, K., S. Kahl, M. Z. Peery, H. Klinck, and C. M. Wood. 2023. Feature embeddings from the BirdNET algorithm provide insights into avian ecology. Ecological Informatics 74:101995.

Melles, S., S. Glenn, and K. Martin. 2003. Urban bird diversity and landscape complexity: species-environment associations along a multiscale habitat gradient. Conservation Ecology 7:5.

Miller, C., and D. L. Urban. 1999. Forest Pattern, Fire, and Climatic Change in the Sierra Nevada. Ecosystems 2:76–87.

Miller, D. A., J. D. Nichols, B. T. McClintock, E. H. C. Grant, L. L. Bailey, and L. A. Weir. 2011. Improving occupancy estimation when two types of observational error occur: non-detection and species misidentification. Ecology 92:1422–1428.

Miller, D. A. W., L. L. Bailey, E. H. C. Grant, B. T. McClintock, L. A. Weir, and T. R. Simons. 2015. Performance of species occurrence estimators when basic assumptions are not met: a test using field data where true occupancy status is known. Methods in Ecology and Evolution 6:557–565.

Miller, D. A. W., K. Pacifici, J. S. Sanderlin, and B. J. Reich. 2019. The recent past and promising future for data integration methods to estimate species' distributions. Methods in Ecology and Evolution 10:22–37.

Mitchell, M. S., R. A. Lancia, and J. A. Gerwin. 2001. Using Landscape-Level Data to Predict the Distribution of Birds on a Managed Forest: Effects of Scale. Ecological Applications 11:1692–1708.

Morelli, T. L., M. T. Hallworth, T. Duclos, A. Ells, S. D. Faccio, J. R. Foster, K. P. McFarland, K. Nislow, J. Ralston, M. Ratnaswamy, W. V. Deluca, and A. P. K. Siren. 2025. Does habitat or climate change drive species range shifts? Ecography 2025:e07560.

Morley, J. W., R. L. Selden, R. J. Latour, T. L. Frölicher, R. J. Seagraves, and M. L. Pinsky. 2018. Projecting shifts in thermal habitat for 686 species on the North American continental shelf. PLOS ONE 13:e0196127.

Noel, A., D. R. Schlaepfer, B. J. Butterfield, M. C. Swan, J. Norris, K. Hartwig, M. C. Duniway, and J. B. Bradford. 2025. Most Pinyon–Juniper Woodland Species Distributions Are Projected

to Shrink Rather Than Shift Under Climate Change. Rangeland Ecology & Management 98:454–466.

Ovaskainen, O. 2002. Long-term persistence of species and the SLOSS problem. Journal of Theoretical Biology 218:419–433.

Pérez-Granados, C., and J. Traba. 2021. Estimating bird density using passive acoustic monitoring: a review of methods and suggestions for further research. Ibis 163:765–783.

Pope, M., M. Hansen, and J. Crawford. 2004. Habitat associations of translocated and native mountain quail in Oregon. Northwest Science.

Ralph, C. J., G. R. Geupel, P. Pyle, T. E. Martin, and D. F. DeSante. 1993. Handbook of field methods for monitoring landbirds. USDA Forest Service/UNL Faculty Publications:105.

Rigge, M., B. Bunde, S. E. McCord, G. Harrison, T. J. Assal, and J. L. Smith. 2025. Spatial Scale Dependence of Error in Fractional Component Cover Maps. Rangeland Ecology & Management 99:77–87.

Riggio, J., A. Engilis, H. Cook, E. de Greef, D. S. Karp, and M. L. Truan. 2023a. Long-term monitoring reveals the impact of changing climate and habitat on the fitness of cavity-nesting songbirds. Biological Conservation 278:109885.

Riggio, J., A. Engilis, H. Cook, E. de Greef, D. S. Karp, and M. L. Truan. 2023b. Long-term monitoring reveals the impact of changing climate and habitat on the fitness of cavity-nesting songbirds. Biological Conservation 278:109885.

Roberts, L. J., R. D. Burnett, A. M. Fogg, and G. R. Geupel. 2011a. Sierra Nevada National Forests Management Indicator Species Project. Final Study Plan and Sampling Protocols for

Mountain Quail (Oreortyx pictus), Hairy Woodpecker (Picoides villosus), Fox Sparrow (Passerella iliaca), and Yellow Warbler (Dendroica petechia). Page 75. PRBO Conservation Science, Petaluma, California, USA.

Roberts, L. J., R. D. Burnett, A. M. Fogg, and G. R. Geupel. 2011b. Final Study Plan and Sampling Protocols for Mountain Quail (Oreortyx pictus), Hairy Woodpecker (Picoides villosus), Fox Sparrow (Passerella iliaca), and Yellow Warbler (Dendroica petechia). PRBO Conservation Science, Petaluma, California, USA.

Roberts, L. J., R. Burnett, J. Tietz, and S. Veloz. 2019a. Recent drought and tree mortality effects on the avian community in southern Sierra Nevada: a glimpse of the future? Ecological Applications 29:e01848.

Roberts, L. J., R. Burnett, J. Tietz, and S. Veloz. 2019b. Recent drought and tree mortality effects on the avian community in southern Sierra Nevada: a glimpse of the future? Ecological Applications 29:e01848.

Rousseau, J. S., and M. G. Betts. 2022. Factors influencing transferability in species distribution models. Ecography 2022:e06060.

Rousseau, J. S., B. Campos, R. Hammond, and R. Burnett. 2025. Sierra Nevada National Forests Avian Management Indicator Species Project: 2024 Annual Report. Page 29. Point Blue Conservation Science, Petaluma, California, USA.

Royle, J. A., R. B. Chandler, C. Yackulic, and J. D. Nichols. 2012. Likelihood analysis of species occurrence probability from presence-only data for modelling species distributions. Methods in Ecology and Evolution 3:545–554.

Royle, J. A., and W. A. Link. 2006. Generalized Site Occupancy Models Allowing for False Positive and False Negative Errors. Ecology 87:835–841.

Saab, V. 1999. Importance of Spatial Scale to Habitat Use by Breeding Birds in Riparian Forests: A Hierarchical Analysis. Ecological Applications 9:135–151.

Salas-Eljatib, C., A. Fuentes-Ramirez, T. G. Gregoire, A. Altamirano, and V. Yaitul. 2018. A study on the effects of unbalanced data when fitting logistic regression models in ecology. Ecological Indicators 85:502–508.

Samiappan, S., B. S. Krishnan, D. Dehart, L. R. Jones, J. A. Elmore, K. O. Evans, and R. B. Iglay. 2024. Aerial Wildlife Image Repository for animal monitoring with drones in the age of artificial intelligence. Database 2024:baae070.

Saracco, J. F., R. B. Siegel, L. Helton, S. L. Stock, and D. F. DeSante. 2019. Phenology and productivity in a montane bird assemblage: Trends and responses to elevation and climate variation. Global Change Biology 25:985–996.

Sauer, J. R., W. A. Link, and J. E. Hines. 2020. The North American Breeding Bird Survey, Analysis Results 1966 - 2019. U.S. Geological Survey.

Shah, K., G. Ballard, A. Schmidt, and M. Schwager. 2020. Multidrone aerial surveys of penguin colonies in Antarctica. Science Robotics 5:eabc3000.

Snyder, R., M. Clark, L. Salas, W. Schackwitz, D. Leland, T. Stephens, T. Erickson, T. Tuffli, M. Tuffli, and K. Clas. 2022. The Soundscapes to Landscapes Project: Development of a Bioacoustics-Based Monitoring Workflow with Multiple Citizen Scientist Contributions. Citizen Science: Theory and Practice 7:24.

Steel, Z. L., G. M. Jones, B. M. Collins, R. Green, A. Koltunov, K. L. Purcell, S. C. Sawyer, M. R. Slaton, S. L. Stephens, P. Stine, and C. Thompson. 2023. Mega-disturbances cause rapid decline of mature conifer forest habitat in California. Ecological Applications 33:e2763.

Steel, Z. L., H. D. Safford, and J. H. Viers. 2015. The fire frequency-severity relationship and the legacy of fire suppression in California forests. Ecosphere 6:art8.

Steenweg, R., M. Hebblewhite, J. Whittington, P. Lukacs, and K. McKelvey. 2018. Sampling scales define occupancy and underlying occupancy–abundance relationships in animals. Ecology 99:172–183.

Stephenson, J. A., K. P. Reese, P. Zager, P. E. Heekin, P. J. Nelle, and A. Martens. 2011. Factors influencing survival of native and translocated mountain quail in Idaho and Washington. The Journal of Wildlife Management 75:1315–1323.

Strang, A. J., E. Z. Cameron, D. P. Anderson, E. Robinson, and M. A. LaRue. 2025. Review of the techniques for estimating population size of Adélie penguins (Pygoscelis adeliae). Polar Biology 48:23.

Stuber, E. F., and L. F. Gruber. 2020. Recent Methodological Solutions to Identifying Scales of Effect in Multi-scale Modeling. Current Landscape Ecology Reports 5:127–139.

Syphard, A. D., S. J. E. Velazco, M. B. Rose, J. Franklin, and H. M. Regan. 2024. The importance of geography in forecasting future fire patterns under climate change. Proceedings of the National Academy of Sciences 121:e2310076121.

Taillie, P. J., R. D. Burnett, L. J. Roberts, B. R. Campos, M. N. Peterson, and C. E. Moorman. 2018. Interacting and non-linear avian responses to mixed-severity wildfire and time since fire. Ecosphere 9:e02291.

Ten Caten, C., L. Holian, and T. Dallas. 2022. Weak but consistent abundance–occupancy relationships across taxa, space and time. Global Ecology and Biogeography 31:968–977.

Thompson, C. M., and K. Mcgarigal. 2002. The influence of research scale on bald eagle habitat selection along the lower Hudson River, New York (USA). Landscape Ecology; Dordrecht 17:569–586.

Thorne, J. H., H. Choe, P. A. Stine, J. C. Chambers, A. Holguin, A. C. Kerr, and M. W. Schwartz. 2018. Climate change vulnerability assessment of forests in the Southwest USA. Climatic Change 148:387–402.

USDA Forest Service. 2008. Sierra Nevada Forests Management Indicator Species Amendment. USDA Forest Service, Region 5, Pacific Southwest Region.

Van Wilgenburg, S. L., P. Sólymos, K. J. Kardynal, and M. D. Frey. 2017. Paired sampling standardizes point count data from humans and acoustic recorders. Avian Conservation and Ecology 12:art13.

Vélez, J., W. McShea, H. Shamon, P. J. Castiblanco-Camacho, M. A. Tabak, C. Chalmers, P. Fergus, and J. Fieberg. 2023. An evaluation of platforms for processing camera-trap data using artificial intelligence. Methods in Ecology and Evolution 14:459–477.

Wilkins, L. G. E., K. R. Matthews, Z. L. Steel, S. C. Nusslé, and S. M. Carlson. 2019. Population dynamics of Rana sierrae at Dusy Basin: influence of non-native predators, drought, and restoration potential. Ecosphere 10:e02951.

Williams, B. K., and E. D. Brown. 2014. Adaptive Management: From More Talk to Real Action. Environmental Management 53:465–479.

Williams, J. N., H. D. Safford, N. Enstice, Z. L. Steel, and A. K. Paulson. 2023. High-severity burned area and proportion exceed historic conditions in Sierra Nevada, California, and adjacent ranges. Ecosphere 14:e4397.

Yu, H., S. Jiang, and K. C. Land. 2015. Multicollinearity in hierarchical linear models. Social Science Research 53:118–136.

Zeller, K. A., N. A. Povak, P. Manley, S. W. Flake, and K. L. Hefty. 2023. Managing for biodiversity: The effects of climate, management and natural disturbance on wildlife species richness. Diversity and Distributions 29:1623–1638.

Zipkin, E. F., S. Rossman, C. B. Yackulic, J. D. Wiens, J. T. Thorson, R. J. Davis, and E. H. C. Grant. 2017. Integrating count and detection–nondetection data to model population dynamics. Ecology 98:1640–1650.

Zuckerberg, B., W. F. Porter, and K. Corwin. 2009. The consistency and stability of abundance–occupancy relationships in large-scale population dynamics. Journal of Animal Ecology 78:172–181.